JAERI-Research
95-069

THE AQUEOUS SOLUBILITY AND SPECIATION ANALYSIS FOR URANIUM, NEPTUNIUM AND SELENIUM BY THE GEOCHEMICAL CODE (EQ3/6)

November 1995

Seiji TAKEDA, Shigeki SHIMA, Hideo KIMURA
and Hideo MATSUZURU

日本原子力研究所
Japan Atomic Energy Research Institute

本レポートは，日本原子力研究所が不定期に公刊している研究報告書です。
入手の問合わせは，日本原子力研究所技術情報部情報資料課（〒319-11 茨城県那珂郡東海村）あて，お申し越しください。なお，このほかに財団法人原子力弘済会資料センター（〒319-11 茨城県那珂郡東海村日本原子力研究所内）で複写による実費頒布をおこなっております。

This report is issued irregularly.
Inquiries about availability of the reports should be addressed to Information Division, Department of Technical Information, Japan Atomic Energy Research Institute, Tokai-mura, Naka-gun, Ibaraki-ken 319-11, Japan.

編集兼発行　日本原子力研究所
印　　刷　㈱原子力資料サービス

The Aqueous Solubility and Speciation Analysis for Uranium, Neptunium and Selenium by the Geochemical Code(EQ3/6)

Seiji TAKEDA, Shigeki SHIMA, Hideo KIMURA
and Hideo MATSUZURU

Department of Environmental Safety Research
Tokai Research Establishment
Japan Atomic Energy Research Institute
Tokai-mura, Naka-gun, Ibaraki-ken

(Received October 2, 1995)

The geochemical condition of a geologic disposal system of HLW controls the solubility and physicochemical forms of dominant aqueous species for elements, which are one of essential information required for safety assessment. Based on the measured compositions of groundwater, the compositions of groundwater in the disposal system were calculated. The solubility and speciation analyses for the polyvalent elements, uranium, neptunium, and selenium, were performed by the geochemical code EQ3/6. The results obtained were compared with the data appeared in the literatures on the solubilities and speciations.

The geochemical behaviors of the elements with respect to the solubility and speciation could quantitatively be elucidated for the compositions of the interstitial waters in an engineered barrier and ground water in a natural barrier. In the pH range of neutral to alkali, the solubilities of U and Np tend to increase with an increase of the carbonate concentration in groundwater. This carbonate concentration dependence of the solubility was also estimated. In the engineered barrier the predominant aqueous species were specified, and in the natural barrier the change of aqueous species was also predicted while the chemical compositions changed from the reducing to oxidizing conditions. The dominant aqueous species for the elements, which migrate in and through the disposal system, were determined by the speciation analysis.

Keywords: Geochemical Model, Geochemistry, Solubility and Speciation Analysis,
Chemical Composition, Eh-pH Condition, Thermodynamic Data, Groundwater,
Uranium, Neptunium, Selenium, Radioactive Waste Disposal,
High-level Radioactive Waste, Safety Assessment

地球化学モデルによるU，Np，Seの溶解度と化学種の解析

日本原子力研究所東海研究所環境安全研究部
武田　聖司・島　茂樹・木村　英雄・松鶴　秀夫

（1995年10月2日受理）

高レベル放射性廃棄物（ＨＬＷ）の処分サイトにおける地球化学的な条件は，深地層処分システムの一般的安全評価に必要とされる放射性元素の溶解度や支配的な溶存化学種に影響を与える。そこで実測された地下水組成から処分サイトの地下水組成の変化を解析し，その組成に対して地球化学コードＥＱ３／６により多価元素であるU，Np，Seの溶解度と化学種の推定を行った。また，各研究機関の溶解度及び化学種に関する報告と解析結果の比較検討を行った。

溶解度の解析から，人工バリア内において想定される地下水の化学特性の変化に対する各元素の溶解度特性を定量的に評価することができた。また，酸化雰囲気の中性あるいはアルカリ側の地下水において炭酸濃度の上昇がU，Npの溶解度の上昇をもたらし，炭酸濃度が溶解度に及ぼす影響の程度を把握することができた。化学種については，人工バリアにおける支配的な溶存化学種が推定でき，天然バリアでは還元雰囲気から酸化雰囲気に地下水特性が変化する間の溶存化学種の変化を予測することができた。この化学種の解析から，処分サイトを移行する際の放射性元素の主要な化学種が特定された。

東海研究所：〒319-11　茨城県那珂郡東海村白方白根２－４

Contents

目　　次

1. INTRODUCTION

In the safety assessment for deep geologic disposal of high-level radioactive waste (HLW), the geochemical condition of the disposal system is one of important factors, which govern the performance of the multibarrier system consisting of engineered and natural barriers. The geochemical condition controls the corrosion of metallic containers (canister and overpack) by an interstitial water in the engineered barrier, determine the dissolution of radionuclides from in a waste form, and also govern a chemical form of radionuclides which migrate through the multibarrier .

Figure 1 shows the relation between the chemical condition of groundwater and parameters involved in radionuclide transport models to be used in the long-term safety assessment. Such parameters as the solubility and the distribution coefficient of elements depend significantly on the groundwater chemical condition. The distribution coefficient of a specific element, which is an equilibrium parameter to define partitioning of a solute between a solid and a liquid phase, will vary with possible chemical forms of the element in an aqueous solution, e.g., cationic, anionic and nonionic forms.

Solubility and thermodynamic data have been obtained from the experiments with solutions of relatively simple compositions compared with natural groundwater. It might be difficult to make the direct estimation, based on these experimental measurements, of their solubilities in solutions containing many kinds of co-ions. The effects of many kinds of aqueous species coexisting in solutions are not negligible to determine the solubility of a specific species. Therefore aqueous solubility and speciation in geochemical environments are subjected to calculations by using geochemical models, based on reliable thermodynamic data obtained from the experiments with solutions of relatively simple compositions. The time durations of these experiments are at the longest a few years. The time scale to consider in the safety assessment is of the orders of at least a few thousand years or more. The change in the long-term chemical compositions in groundwater must be predicted.

Considering the circumstances mentioned above, based on the measured characteristics of the deep groundwater, the solubility and speciation analyses for some kinds of the groundwater have been undertaken by SKI (Swedish Nuclear Power Inspectorate, Sweden)[1] and SKB (Swedish Nuclear Fuel and Waste Management Co., Sweden)[2]. Chemical interactions between solutions and minerals under physical and chemical conditions of a deep geologic environment can be modeled by the geochemical code, e.g., PHREEQE[3] and EQ3/6[4]. The geochemical code must be supported by thermodynamic data, and the reliability of the analyzed results of solubility and speciation thereby depends on the credibility of the thermodynamic data. The thermodynamic data of some kinds of elements have been collected by OECD/NEA. Most of the thermodynamic data used here were obtained from OECD/NEA, and were selected by the criterion of thereliable data used in many literatures. Reacent literatures concerning thermodynamic data of elements

were also cited.

In this report, the aqueous solubility and speciation of several polyvalent elements were analyzed by the geochemical code system EQ3/6 by assuming the thermodynamic equilibrium, under some chemical conditions of the groundwater, which are expected in near and far fields. Considering the space- and time-varying chemical characteristic of the groundwater, two types of models for the groundwater were assumed. For the first model (Model 1), the chemical compositions of the interstitial water in the engineered barrier under the reducing conditions were assumed, and for the second model (Model 2), the granitic groundwater in the natural barrier. These chemical compositions were calculateded by the geochemical code by assuming the thermodynamic equilibrium, based on the measured compositions of groundwater. The results obtained here were compared with the literatures on solubility and speciation.

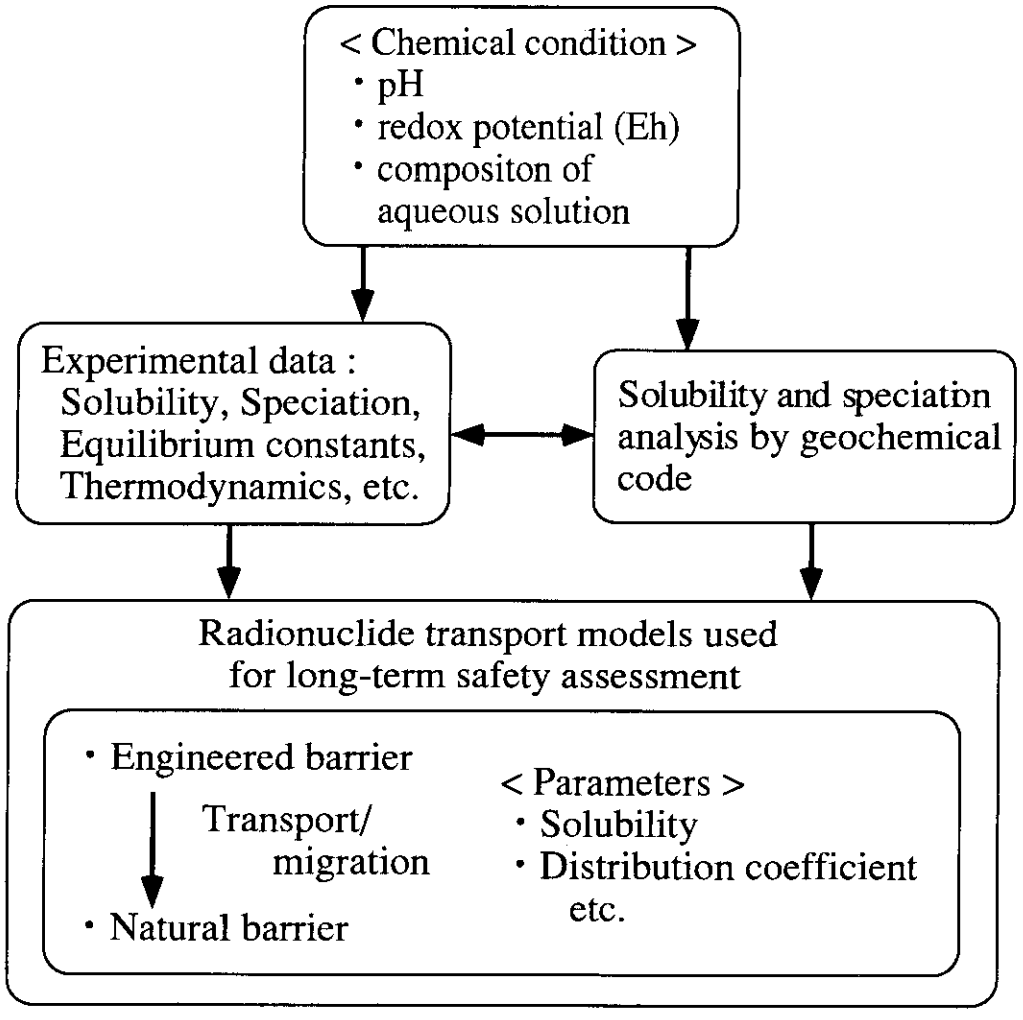

Fig. 1 Relation between chemical conditions in groundwater and radonuclide transport models used for long-term safety assessment

2. GEOCHEMICAL MODEL

2.1 Geochemical Code

The geochemical software package EQ3/6 (version 3245) [4][5][6] consists of main two kinds of the geochemical codes, the EQ3NR code and the EQ6 code, and is supported by the thermodynamic data base and the conversion programs for this data base. It is possible for EQ3/6 to model geochemical processes such as chemical interactions between water-solid or water-mineral. The geochemical code EQ3/6 has been used in the solubility and speciation analyses for many aqueous environments, and known as the code with a high reliability.

The flow of information between data files and codes for the EQ3/6 package is shown in Fig. 2. The MCRT code builds the equilibrium constants for aqueous species, minerals, and gases from the thermodynamic data base, and the output file is given as a text form. The EQPT is the preprocessor for the EQ3/6 data base, and the input of the EQPT code is the output of MCRT. Based on the thermodynamic data, concentrations and abundances of individual aqueous species are calculated by the Newton-Raphson method. In the EQ3/6 package, the degree of nonequilibrium for each chemical reaction is estimated by either the saturation index or the thermodynamic affinity for each mineral.

$$SI=\log (Q/K) \tag{1}$$

where

SI : Saturation index for a mineral

Q : Activity product for a dissolution reaction

K : Equilibrium constant for a dissolution reaction

$$A= -2.303\ RT \log (Q/K) \tag{2}$$

where

A : Thermodynamic affinity

R : The gas constant

T : Kelvin temperature

Following these conventions, both SI and A are positive for supersaturated minerals, zero for saturated minerals, and negative for undersaturated minerals.

The input of the EQ3NR code must contain the compositions of groundwater such as pH, redox-potential (Eh), concentration of each element, and so on. Chemical reactions involved in geochemical processes are assumed to obey either the thermodynamic equilibrium or chemical kinetic theory. The speciation of elements in solutions is estimated by the EQ3NR code by assuming the thermodynamic equilibrium. The EQ6 code deals with the two kinds of models, thermodynamic equilibrium model and kinetic model. The former calculates the speciation and

the quantity of a specific species in a liquid, solid, and gas phase. The later makes reaction-path calculations based on the kinetic theory. A major obstacle to reliable kinetic reaction path modelling is the lack of kinetic data. Present understanding of chemical kinetics is far inferior to that of thermodynamics. The EQ6 code needs the data files which are initialized by the EQ3NR calculation. Model type, reactants, and physical conditions such as temperature and pressure are selected as the input data of EQ6.

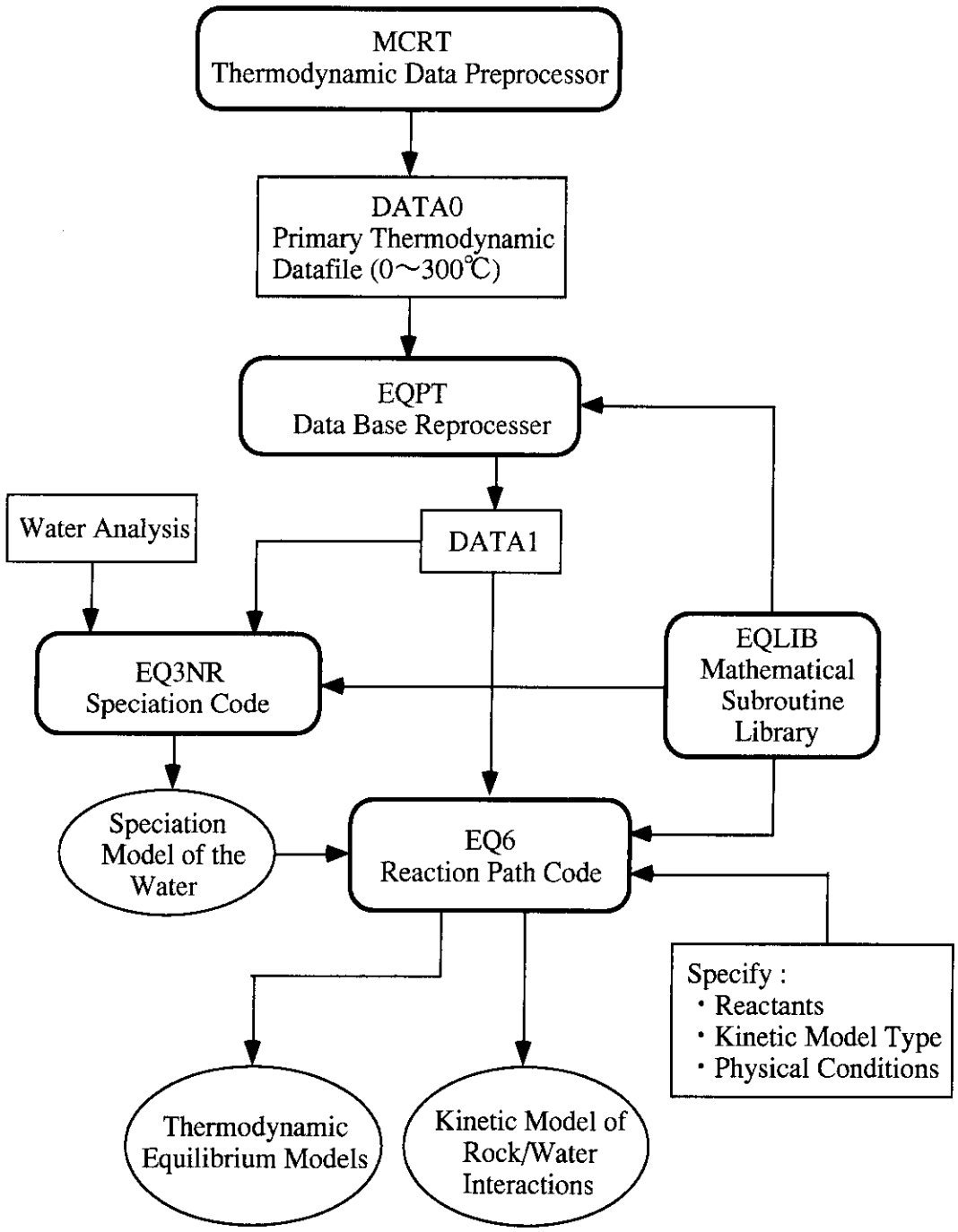

Fig. 2 Flow of information between datafiles and codes for the EQ3/6 package

2.2 Methodology of Analysis

The site selection for disposal of nuclear wastes generally requires radiological information obtained through a preliminary safety assessment for the reasonable conditions including geochemical condition of groundwater, geological structure, hydrologic condition. These conditions affecting the performance of a disposal system depend on characteristics of specific disposal sites, and the prediction of these conditions provides with scientific bases upon which the long-term safety assessment is conducted. From viewpoints of the long-term performance assessment of the engineered barrier and migration modelling in the natural barrier, geochemical conditions are of great importance.

In this study, the chemical composition of groundwater in a postulated disposal site was assumed as follows. The composition of groundwater is characterized by a kind of rock mass which constitutes the disposal site, and the composition measured in a specific rock, granite, was used as the standard chemical conditions. Two kinds of the chemical composition were used in the study as shown in Fig. 3; the interstitial water in the engineered barrier and the groundwater flowing through the natural barrier. The reason of this is that the processes by which the chemical composition of groundwater changes with time in the engineered barrier might differ from those in the natural barrier. In the engineered barrier, the chemical composition of the interstitial water will be changed by the chemical interactions between the engineered barrier materials and the water. This change in the composition of the interstitial water might have an effect on the dissolution process of the vitrified matrix and also the migration of radionuclides in the engineered barrier. The vitrified matrix confines radionuclides, however, once the container failed significantly the matrix will dissolve by contacting with groundwater which permeates into the engineered barrier. Radionuclides thus released are transported by diffusion in the engineered

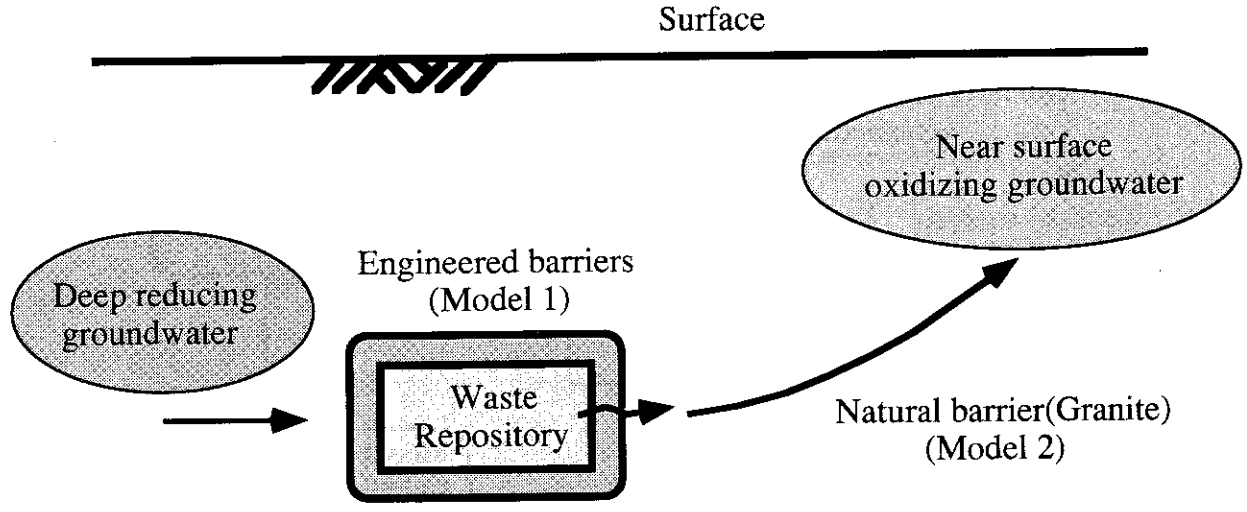

Fig. 3 Analysis cases of the aqueous solubility and speciation
Model 1: in interstitial water of the engineered barriers (reducing environments)
Model 2: in groundwater of the natural barrier (reducing→oxidizing environments)

barrier. In the natural barrier, radionuclides leaking out from the engineered barrier will be transported by the groundwater flow to a far field. Along this transport pathway, the chemical conditions might be changed from the reducing condition in a deep geosphere to the oxidizing conditions in the surface layer. This change in the groundwater characteristics will influence the migration mechanisms of radionuclides in the natural barrier.

The chemical compositions in the engineered and the natural barriers were determined by the analyses with the geochemical models as shown in Fig. 4. A methodology used for the analyses of geochemical processes is either the thermodynamic equilibrium modelling or the kinetic modelling. Considering that the groundwater velocity in buffer materials of a multibarrier system is extremely low, the time scale for chemical interactions between the materials constituting these barriers and groundwater will be long enough to be in equilibrium. The geochemical processes might be approximately described by the thermodynamic equilibrium modelling. Based on the equilibrium models, the interstitial water compositions in the engineered barrier were determined by the chemical reactions between the initial deep groundwater and the engineered barrier materials such as an overpack and buffer material. The subsequent analyses used the equilibrium compositions of the interstitial water in which each component stably coexists with their materials, but excludes the use of the initial transient composition which changes with time. The chemical compositions of the interstitial water in the engineered barrier were determined by the use of analyses by assuming the conditions that the deep groundwater is in contact with the buffer material (bentonite) and magnetite (main corrosion product)[7]. The chemical compositions of

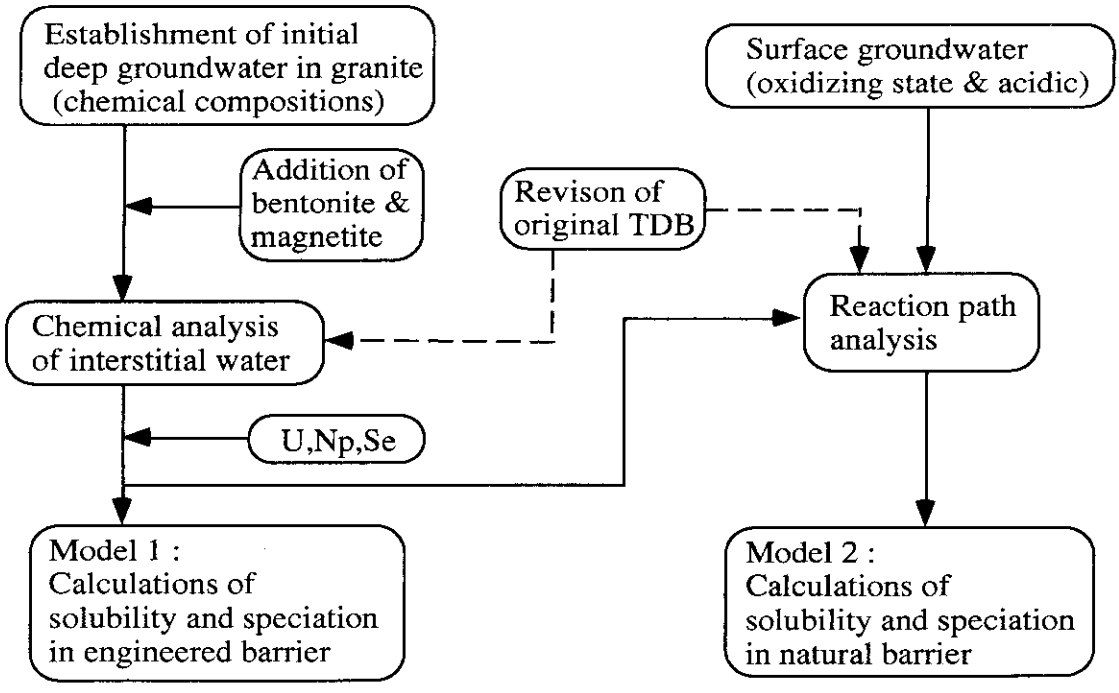

Fig. 4 Flow chart for calculations of solubility and speciation

groundwater in the natural barrier were analyzed with the geochemical code by assuming that in the natural barrier the mixing occurs between the interstitial water coming from the engineered barrier and the oxidizing groundwater in the surface layer. Under the conditions of those compositions thus determined, the solubility and speciation for elements were analyzed by the geochemical code EQ3/6. This report deals with three elements, uranium, neptunium, and selenium, which belong to the group of nuclides with high potential radiological consequences. These elements have three or four kinds of the oxidation states, and are assumed to show complicated behaviors in the disposal system depending on the chemical conditions in each barrier.

2.3 Chemical Composition of Groundwater

The chemical compositions of groundwater measured in both reducing and oxidizing granitic zone[8], which widely distributes in Japan, were used here as the standard. These compositions of the groundwater were measured to depth of 300m. The standard compositions of the natural granitic groundwater are shown in Table 1. The chemical composition of the deep groundwater was determined as the average of the reducing groundwaters measured at about 100 m in depth, and that of the oxidizing groundwater was inferred from the measured compositions of the groundwater in a near surface, but the redox-potential (Eh) is not given in the measured

Table 1 Chemical compositions of the natural granitic groundwater

	Deep reducing groundwater	Oxidizing groundwater near surface
pH	6.7	4.0
Eh (mV)	-200	500
Alkalinity(eq/l)	0.002	-
Fe (mg/l)	1.20	0.50
Na (mg/l)	14.3	6.50
K (mg/l)	1.50	0.95
Ca (mg/l)	11.5	7.80
Mg (mg/l)	3.50	1.60
Cl (mg/l)	14.5	6.60
NO_3^- (mg/l)	0.01	0.94
SO_4^{2-} (mg/l)	2.20	18.6
SiO_2(aq) (mg/l)	31.0	21.7

compositions. In fact, there are a few descriptions of the redox-potential in the measured data of Japanese groundwater. The redox-potential for the deep granitic groundwater have been measured abroad. The redox-potential of - 200 mV was assumed here based on these measured data. It was assumed that the Eh-pH of the oxidizing groundwater in the natural barrier distributes over a wide range. The redox-potential to be used here for the standard oxidizing groundwater in a near surface was determined based on Eh data of acid precipitation.

The Eh-pH ranges for Model 1 and Model 2, which are calculated from two kinds of the standard compositions, are shown in Fig. 5. In the Eh-pH range calculated for Model 1, bentonite and magnetite contact with the deep reducing groundwater. The compositions of the interstitial water in the engineered barrier were calculated by using the EQ6 code. The analysis with Model1 was performed under the conditions of pH range from pH 6.7 to 10.3. The result of analysis for the composition of the interstitial water at pH 9.1 is shown in Table 2, together with that measured in bentonite-granitic groundwater system[9]. Comparison between them indicates that the composition analyzed here is in a fairly good agreement with the measured composition, although a significant difference in the concentrations of sulfur and iron is observed between them. The difference in the concentration of sulfur between them might be ascribed to the difference in the

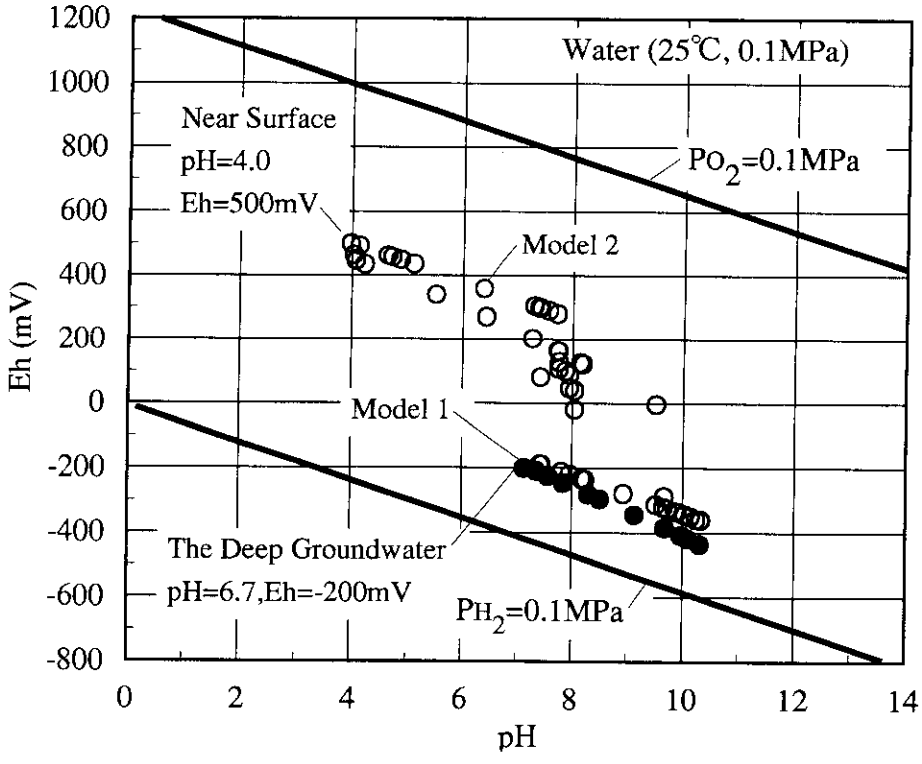

Fig. 5 Eh-pH range of aqueous environments in the engineered barriers (Model 1) and Eh-pH pathway of aqueous environments in the natural barrier (Model 2)

Table 2 Comparison between the calculated interstitial water in the engineered barriers and experimental results

	Interstitial water in engineered barriers	Experimental results (540day)
pH	9.1	9.2
Eh (mV)	-372	-300
HCO_3^-(mol/l)	2.9E-3	6.6E-3
Fe (mol/l)	2.1E-10	1.4E-6
Na (mol/l)	6.9E-3	1.1E-2
K (mol/l)	3.7E-5	6.9E-5
Ca (mol/l)	3.9E-6	2.8E-4
Mg (mol/l)	2.3E-5	1.5E-4
Cl (mol/l)	4.0E-4	1.9E-3
SO_4^{2-} (mol/l)	2.6E-9	6.2E-5
SiO_2(aq) (mol/l)	2.3E-5	2.5E-4

redox potential; - 372 mV obtained by the analysis made here and - 300 mV measured in the experiment, respectively. The higher concentration measured for iron might be ascribed to that the sample containing suspension of iron was not filtered in the experiment. The Eh-ph pathway for Model 2 is shown in Fig. 5. In this figure, the interstitial water in the engineered barrier is the initial condition, and pH decreases and Eh increases due to the mixing with the oxidizing acidic groundwater in the surface layer. The Eh-pH pathway also shows the results of calculations, by using the EQ6 code, for the interaction between the reducing alkaline interstitial water and the oxidizing acidic groundwater. It was assumed that the compositions in the natural barrier are determined by the mixing ratio of two kinds of water and each element, uranium, neptunium, or selenium is mixed at the same time.

2.4 Thermodynamic Data

The thermodynamic data base (TDB) which supports the geochemical code EQ3/6 is of great importance as it dominates the reliability of analytical results. The data base consists of;

- molecular weighs of aqueous species, minerals and gases,
- stoichiometric coefficients of substances involved in chemical reactions, and
- thermodynamic functions.

The thermodynamic data of important species for the elements used here and common minerals were reviewed to prepare data file needed for calculations. The NEA thermodynamic data base[10] has been developed based on a number of literatures concerning thermodynamic data of many elements. In this study, the thermodynamic data for main elements were mostly cited from NEA-TDB. The thermodynamic data of uranium, neptunium, and selenium were given, together with their literatures cited, in appendix of this report.

The Eh-pH diagram of the system U-O-H, which is formed from the thermodynamic data of uranium, is shown in Fig. 6. This figure shows the dominant aqueous species of uranium and the stable range of water at 298.15K and 0.1 MPa. In natural groundwater, uranium has oxidation states ranging from IV to VI. The dominant aqueous species are hydroxy complexes of U(IV) under the reducing conditions, and UO_2^{2+} or its hydroxy complexes in hexavalent state under the oxidizing conditions. The existence of hydroxy complexes of U(IV), $U(OH)_2^{2+}$ and $U(OH)_3^{+}$ is

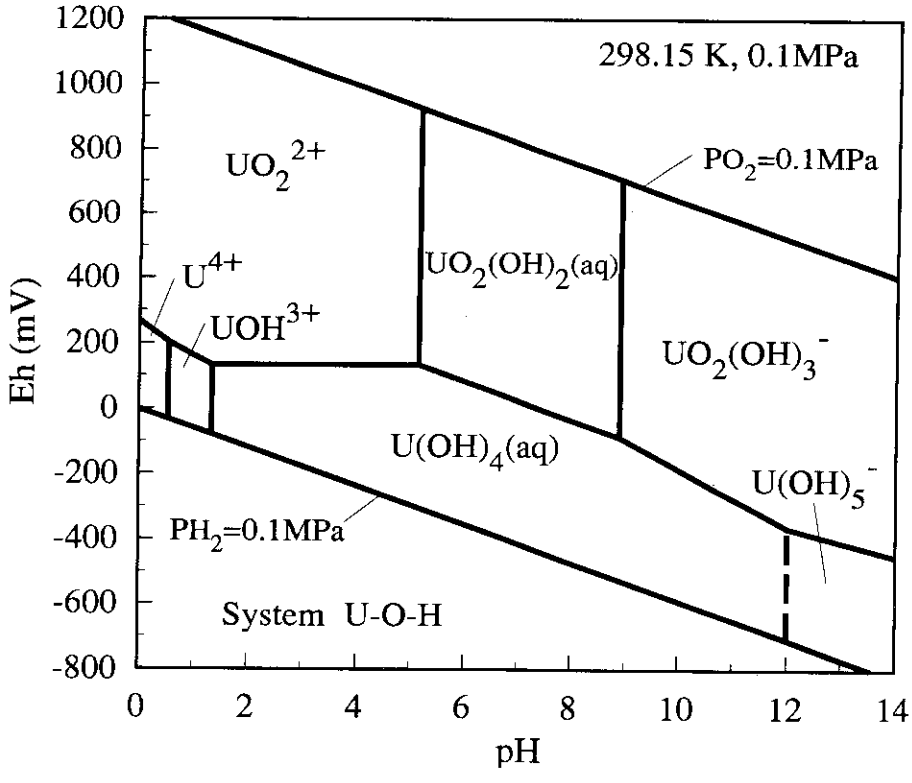

Fig. 6 Eh-pH diagram of the system U-O-H

ambiguous[11], and then these hydroxy complexes were withdrawn from the thermodynamic data base used here. As no evidence of $U(OH)_5^-$ is observed below pH12[11], the dotted line represents the boundary for the predominant range of $U(OH)_5^-$. UO_2^+ or its hydroxy complexes in pentavalent state is unstable in an aqueous solution, resulting in the disproportionation[11]. The Eh-pH diagram of the system U-C-O-H is shown in Fig. 7. In the oxidizing environment, the aqueous species of uranium in hexavalent state exist as carbonate complexes more dominantly than hydroxy complexes. Figure 7 which gives diagrams for both concentrations of carbonate, 10^{-2} and 10^{-3} mol/l, suggests that the region in which carbonate complexes exist dominantly widens with the increase in the carbonate concentration. Rai, D. et al reported that the solubility of U(IV) hydrous oxides increases dramatically in both high biocarbonate and carbonate solutions and mixed hydroxide carbonate complexes of U(IV) may be dominant in the system U-C-O-H[27]. But experimental information of U(IV) in the system U-C-O-H has hardly been reported. Mixed hydroxide carbonate complexes of U(IV) can not be identified correctly. The solubility and speciation of uranium were calculated without mixed hydroxide carbonate/bicarbonate complexes of U(IV).

The Eh-pH diagram of neptunium in the system Np-O-H is shown in Fig. 8. Neptunium

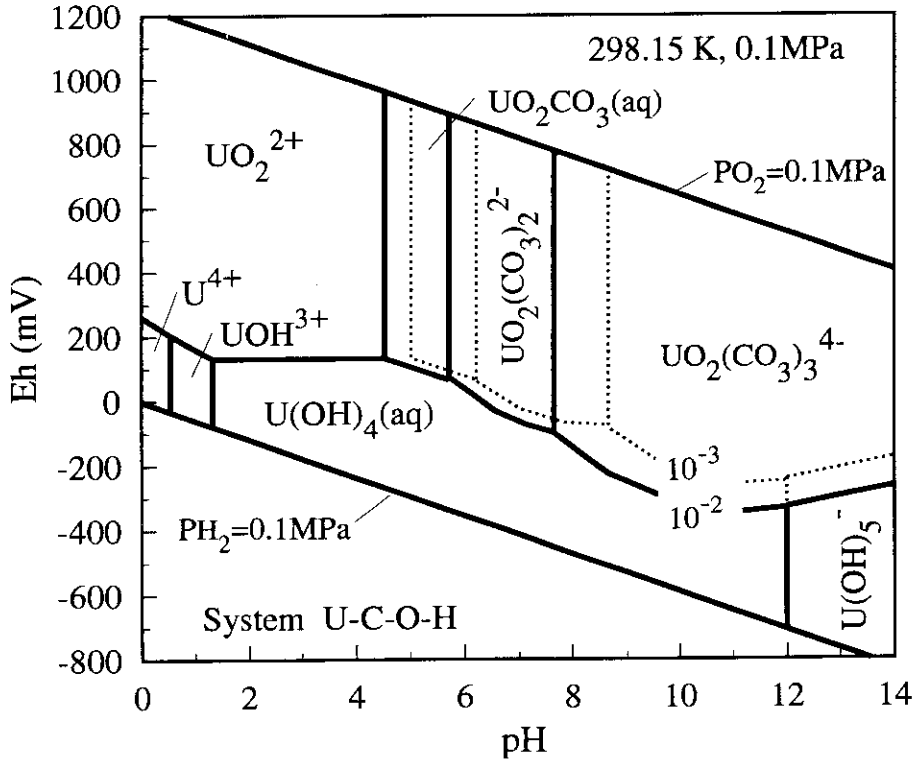

Fig. 7 Eh-pH diagram of the system U-C-O-H
interrupted line: total carbonate concentration $C_T=10^{-3}$ mol/l
solid line: $C_T=10^{-2}$ mol/l

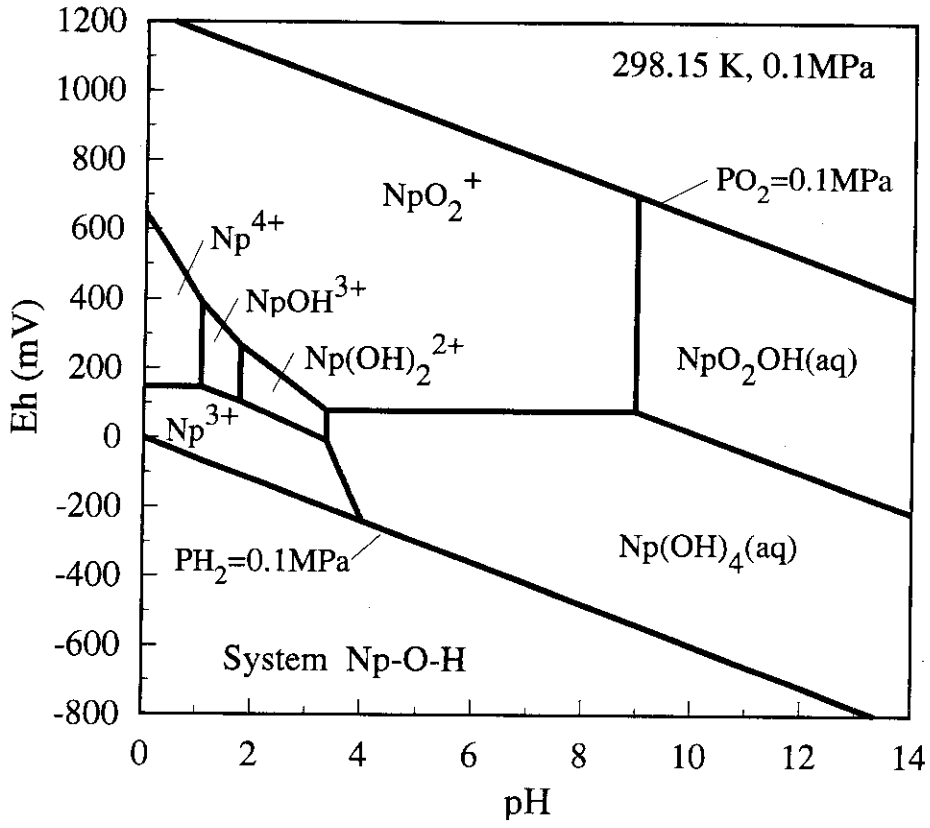

Fig. 8 Eh-pH diagram of the system Np-O-H

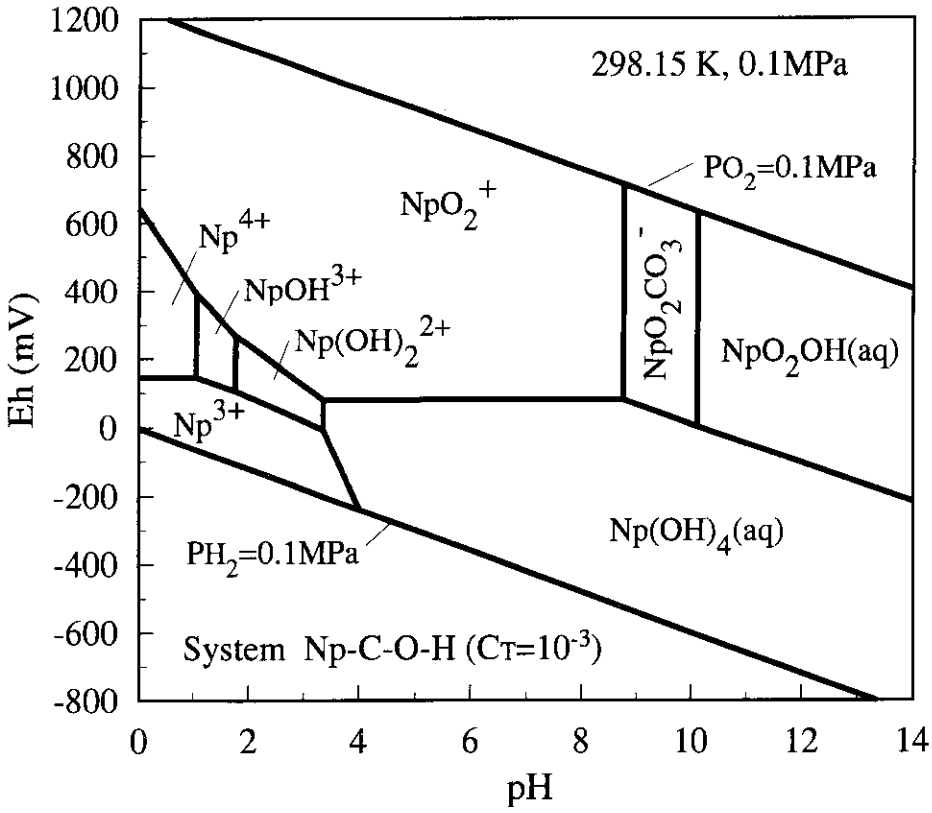

Fig. 9 Eh-pH diagram of the system Np-C-O-H
total carbonate concentration C_T=10^{-3} mol/l

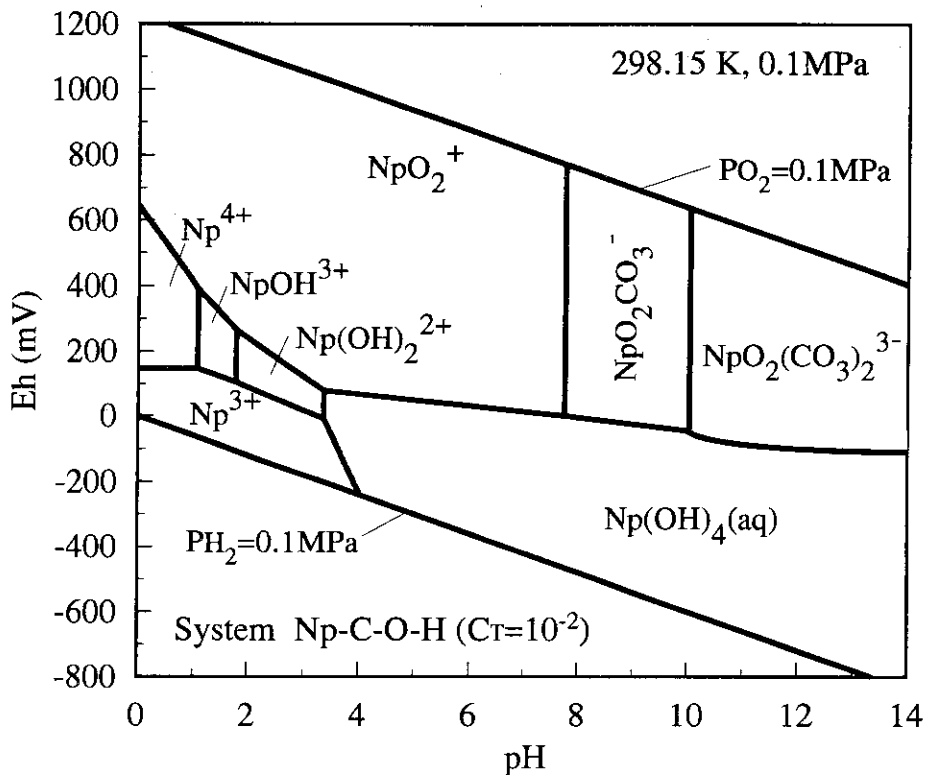

Fig. 10 Eh-pH diagram of the system Np-C-O-H
total carbonate concentration C_T=10^{-2} mol/l

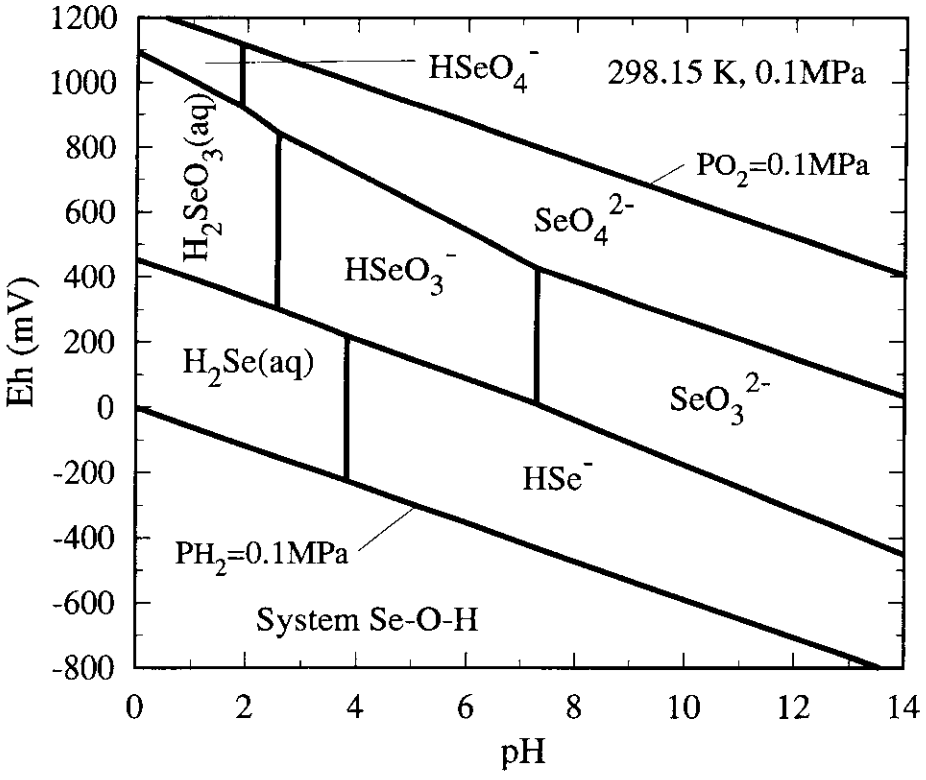

Fig. 11 Eh-pH diagram of the system Se-O-H

exhibits well characterized oxidation states from III to VII, but has the stable oxidation states from IV to VI in natural groundwater. Aqueous chemistry of neptunium resembles that of uranium, but neptunium differs markedly from uranium in that neptunium has a wider stable region of pentavalent state than uranium. In the reducing environments hydroxy complexes of Np(IV) predominate, and in the oxidizing environments species of Np(V). There is a doubt that $Np(OH)_5^-$ predominates in aqueous solutions. Upon studying the solubility of Np(IV), Ray et al.[16] founded no evidence showing the existence of $Np(OH)_5^-$, and assumed the range of the standard molar Gibbs free energy for the formation of $Np(OH)_5^-$ so as to meet experimental evidences obtained. In this study, the standard molar Gibbs free energy for $Np(OH)_5^-$ was cited from this literature[15]. There is no experimental evidence that $Np(OH)_3^+$ is formed in the system Np-O-H, and this species has also been dropped from the data base[12]. Two kinds of the Eh-pH diagrams of the system Np-C-O-H are shown in Figs. 9 and 10 for the total carbonate concentrations of 10^{-3} and 10^{-2} mol/l respectively. In case of the carbonate concentration of 10^{-3} mol/l, the hydroxy complex NpO_2OH (aq) is more predominant than carbonate complexes under the oxidizing and highly alkaline condition, as shown in Fig. 9. As the carbonate concentration increases up to 10^{-2} mol/l, the carbonate complex $NpO_2(CO_3)_2^{3-}$ predominates. Some chemical informations of carbonate complexes of Np(IV) have been reported. From the study of Np(IV) solubility in a carbonate solution, Pratopo, M. I. et al deduced that below pH 10 the species $Np(OH)_2(CO_3)_2^{2-}$ or $Np(OH)_4(CO_3)_2^{4-}$ is predominant in solution, while at pH greater than 11 $Np(OH)_4(CO_3)_2^{4-}$ is predominant[28]. Eriksen, T. E. et al reported that the experimental data of Np(IV) solubility in a carbonate solution are explained by the predominant species, $Np(OH)_3CO_3^-$ and $Np(OH)_4CO_3^{2-}$ [29]. The solubility and speciation analysis were performed without the thermodynamic data of the carbonate complexes of Np(IV) because the carbonate complexes of Np(IV) were not identified. But the effects of carbonate ion in Np(IV) solubility may be significant for the safety assessment of HLW.

The Eh-pH diagram of system Se-O-H is shown in Fig. 11. Selenium can exist in a natural groundwater system as the oxidation states, -II, 0, IV, and VI. There are significant similarity in aqueous chemical behavior between selenium and sulfur. The dominant aqueous species of Se are selenide(-II), selenite(IV), and selenate(VI) depending on the redox potential of an aqueous solution. Some kinds of compounds between metal elements and selenium in each oxidation state are observed.

2.5 Solid Phase in Natural Groundwater

A knowledge about the solid phases of elements that might form in a natural groundwater system is of prime importance in calculations of solubilities. In the safety assessment the solubility of an element is widely used as a parameter to calculate the release flux of radionuclides from the engineered barrier, and depends significantly on possible stable solid phases. Often the solid phase is initially precipitated in a more or less amorphous state, and only very slowly the amorphous phase transforms into the thermodynamically stable crystalline state. The solubility of the amorphous solid is much higher than that of the crystal. The stable solid phases in natural groundwater are a hydroxide, oxide, carbonate, sulfate, fluoride, and phosphate. Fundamental parameters such as Eh-pH conditions, temperature, and groundwater compositions influence these solid phases. Owing to the uncertainty in determinations of the solubility limiting solid phase, the solid phases of uranium, neptunium, and selenium were assumed, taking into account of scientific knowledge obtained from literatures and the thermodynamic data of their solid phases.

Under the reducing conditions UO_2 is the stable solid phase of uranium, but the solubility of UO_2 depends on its particle size or crystallinity. Oxides of uranium in tetravalent state are divided into UO_2(am), UO_2(fuel), and uraninite according to their different characteristics. Uraninite

Table 3 Solubility limiting solid phases of uranium, neptunium and selenium under the reducing and oxidizing conditions (＊: not defined, －: not calculated)

	Uranium		Neptunium		Selenium		
	reducing	oxidizing	reducing	oxidizing	reducing	oxidizing	Ref.
SKI	UO_2	schoepite	$Np(OH)_4$(s)	$Np(OH)_4$(s)	Se(c)	$CaSeO_3$(c)	(1)
SKB	UO_2(fuel)	$UO_2(OH)_2$(c)	$Np(OH)_4$(s)	NpO_2OH(s) $NaNpO_2CO_3$(c)	Fe_3Se4(c)	＊	(2)
YJT	UO_2(fuel)	schoepite	$Np(OH)_4$(s) NpO_2(c)	$Np(OH)_4$(s) NpO_2OH(c) $NaNpO_2CO_3$(c)	Se(c) $FeSe_2$(c)	Se(c)	(34)
PNC	UO_2(c) UO_2(am)	-	$Np(OH)_4$(s) NpO_2(c)	-	Se(c) $FeSe_2$(c)	-	(7)
AERE	UO_2(c) UO_2(am)	-	$Np(OH)_4$(s) NpO_2(c)	-	-	-	(35)

corresponds to well-crystallized UO_2(c), and UO_2(fuel), which is involved in a spent nuclear fuel and has the average particle size of 1 - 5 μm, is an intermediate solid between UO_2(am) and UO_2(c)[30]. The solubility limiting phases of uranium, neptunium, and selenium under the reducing and oxidizing conditions, which appear in the literatures referred here, are summarized in Table 3. The stable solid phases of U in the reducing environments are three kinds of UO_2 mentioned above, however, OECD/NEA[11] excludes thermodynamic data of amorphous UO_2 and its hydrates because of their insufficient reliabilities. Under the oxidizing conditions the solubility of uranium is not controlled by UO_2 in any forms, but by the solid phases of U(VI). These stable solid phases are $UO_2(OH)_2$(c) and schoepite ($UO_3 \cdot 2H_2O$) as shown in Table 3. The experimental study[31] showed that hydroxides of U(VI) is stable at 25℃ and $UO_2(OH)_2$(c) at temperatures higher than 60℃. In the oxidizing environments, the solid phases of U, other than hydroxides, are mixed valence oxides which are composed of U(IV) and U(VI). In the reaction path analysis and the experimental observations, the following sequence for the alteration products of UO_2 was suggested in the presence of atmospheric oxygen; $UO_2 \rightarrow U_4O_9(c) \rightarrow U_3O_7(c) \rightarrow U_3O_8(c) \rightarrow UO_2(OH)_2(c)$[32].

The stable solid phases of neptunium in the reducing environments are both oxides and hydroxides. The experimental study on NpO_2(c) indicates that amorphous $NpO_2 \cdot xH_2O$ may be crystallized within one month[33]. The solid phases of Np under the oxidizing conditions were assumed here to be $Np(OH)_4$(s), NpO_2OH(s) and $NaNpO_2CO_3$(c), as shown in Table 3. $NaNpO_2CO_3$(c) is assumed in SKB[2] and VJT[34] reports the other solid phase for saline groundwater compositions containing NaCl of a high concentration.

Under the reducing conditions, either elemental Se or metal-selenide minerals (Cu_2Se(c), PbSe(c)), has been observed in soils[36]. SKB[2] and YJT[34] decided the solid phase of Se, based on the fact that the solubility of Se is limited by the precipitation of selenides, particularly of Fe, Cu, Pb and Ni, under the reducing conditions. Se^{2-} forms very insoluble compounds with these metal ions. Considering that the interstitial water in the engineered barrier includes Fe, it is reasonable to assume that Se forms $FeSe_2$(c) and Fe_3Se_4(c) in addition to Se(c) as shown in Table 3. In strongly acidic soils, $MnSeO_3$(c) is the only selenite mineral, and other selenite minerals appear to be too soluble to form the stable solid phase in soils particularly in the alkaline pH range[36], while under the oxidizing conditions $CaSeO_3$(c) was assumed as the solubility limiting solid phase of Selenium in SKI[1]. The stable solid phases in the oxidizing environments were inferred to be the compounds formed by metal ions and SeO_3^{2-}.

The thermodynamic data of amorphous UO_2 and NpO_2(c) are widely scattered among the relevant literatures published. These thermodynamic data are shown in Table 4. The solubility measurements of $UO_2 \cdot xH_2O$ in acidic media were reported by Rai, D. et al[37], while the electrochemical measurements of the aged amorphous UO_2 were reported by Bruno, J. K. et al[38]. The preliminary solubility analysis of amorphous UO_2 in the reducing condition is in the range of 4×10^{-5} to 10^{-2}mol/l. The standard molar Gibbs free energy data for the formation of NpO_2(c) in

Table 4 Uncertainty of the thermodynamic data for both amorphous UO_2 and $NpO_2(c)$

solid phase	standard molar Gibbs free energy (kcal/mol)	calculated solubility (mol/l)	references
amorphous UO_2	-233.529	$1x10^{-2}$	(37)
	-239.887	$4x10^{-5}$	(38)
$NpO_2(c)$	-244.229	$5x10^{-18}$	(12)
	-233.588	$3x10^{-10}$	(15)

Table 5 Solubility limiting solid phases used in calculation of Model 1

	reducing conditions		
	Uranium	Neptunium	Selenium
solid phase	$UO_2(c)$	$Np(OH)_4(s)$	$Se(c)$, $FeSe_2(c)$

Lemire, R. J. et al[12] and Wanner, H.[15] contain the differences more than 11 kcal/mol. The preliminary solubility analysis indicated that this discrepancy of thermodynamic data results in the solubility of $NpO_2(c)$ thus calculated being in the range of $5x10^{-18}$ to $3x10^{-10}$mol/l. It is said that there is a large uncertainty of the thermodynamic data for both amorphous UO_2 and $NpO_2(c)$. The solubility limiting solid phases of Model 1 under the reducing conditions are shown in Table 5. The solid phases of selenium were assumed to be Se(c) and $FeSe_2(c)$. The chemical composition of the natural groundwater for Model 2 varies from the reducing to oxidizing condition, resulting in the change of the stable solid phases. The solubility limiting solid phases for the three elements in the natural barrier were not specifically decided, therefore, and the solubility was calculated under the oxidizing condition with respect to the solid phase that was indicated to be the most stable through geochemical computations with changing the chemical composition of groundwater.

3. RESULTS OF ANALYSIS

3.1 Uranium

The results of the solubility and speciation analyses by using Model 1 are given in Fig. 12. The solubility of uraninite, $UO_2(c)$, is constant at $4x10^{-10}$ mol/l, suggesting that the change in chemical composition of the interstitial water dose not influence the solubility of uraninite. The

Table 4 Uncertainty of the thermodynamic data for both amorphous UO_2 and NpO_2(c)

solid phase	standard molar Gibbs free energy (kcal/mol)	calculated solubility (mol/l)	references
amorphous UO_2	-233.529	$1x10^{-2}$	(37)
	-239.887	$4x10^{-5}$	(38)
NpO_2(c)	-244.229	$5x10^{-18}$	(12)
	-233.588	$3x10^{-10}$	(15)

Table 5 Solubility limiting solid phases used in calculation of Model 1

	reducing conditions		
	Uranium	Neptunium	Selenium
solid phase	UO_2(c)	$Np(OH)_4$(s)	Se(c), $FeSe_2$(c)

Lemire, R. J. et al[12] and Wanner, H.[15] contain the differences more than 11 kcal/mol. The preliminary solubility analysis indicated that this discrepancy of thermodynamic data results in the solubility of NpO_2(c) thus calculated being in the range of $5x10^{-18}$ to $3x10^{-10}$mol/l. It is said that there is a large uncertainty of the thermodynamic data for both amorphous UO_2 and NpO_2(c). The solubility limiting solid phases of Model 1 under the reducing conditions are shown in Table 5. The solid phases of selenium were assumed to be Se(c) and $FeSe_2$(c). The chemical composition of the natural groundwater for Model 2 varies from the reducing to oxidizing condition, resulting in the change of the stable solid phases. The solubility limiting solid phases for the three elements in the natural barrier were not specifically decided, therefore, and the solubility was calculated under the oxidizing condition with respect to the solid phase that was indicated to be the most stable through geochemical computations with changing the chemical composition of groundwater.

3. RESULTS OF ANALYSIS

3.1 Uranium

The results of the solubility and speciation analyses by using Model 1 are given in Fig. 12. The solubility of uraninite, UO_2(c), is constant at $4x10^{-10}$ mol/l, suggesting that the change in chemical composition of the interstitial water dose not influence the solubility of uraninite. The

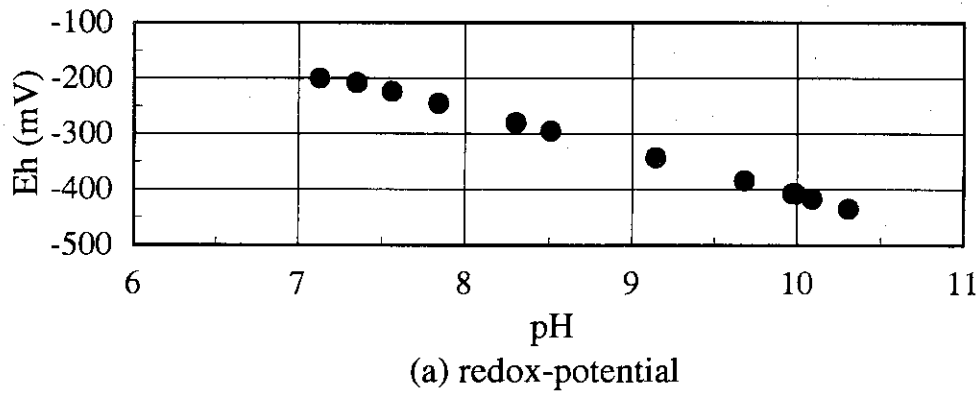

(a) redox-potential

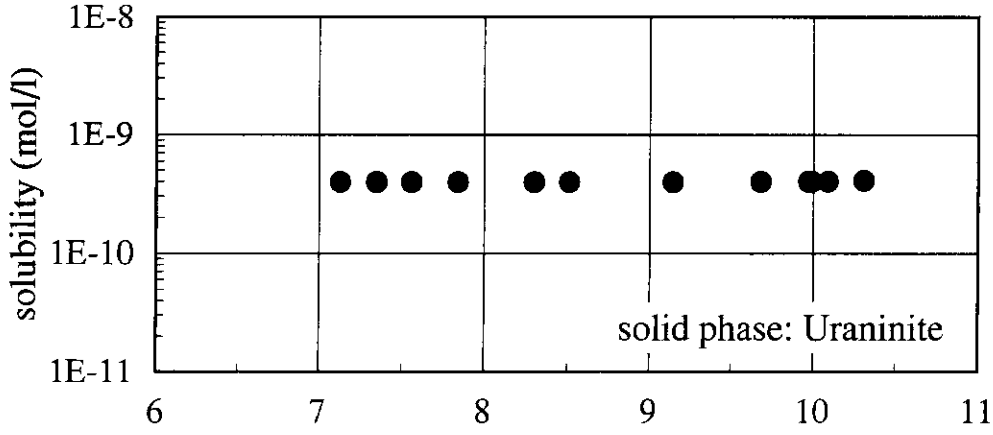

(b) solubility

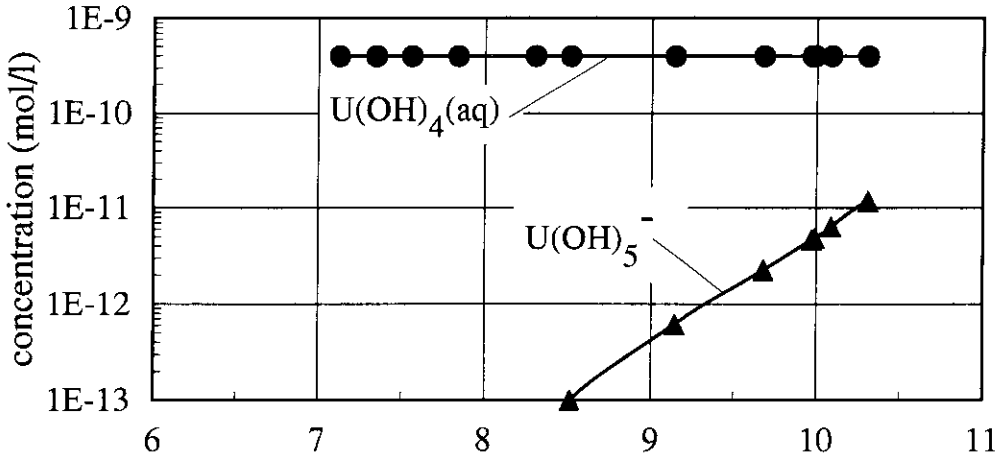

(c) speciation

Fig. 12 Solubility and speciation of uranium in the engineered barrier (reducing environments)

Table 6a Literature data on soubility and speciation of uranium under reducing conditions

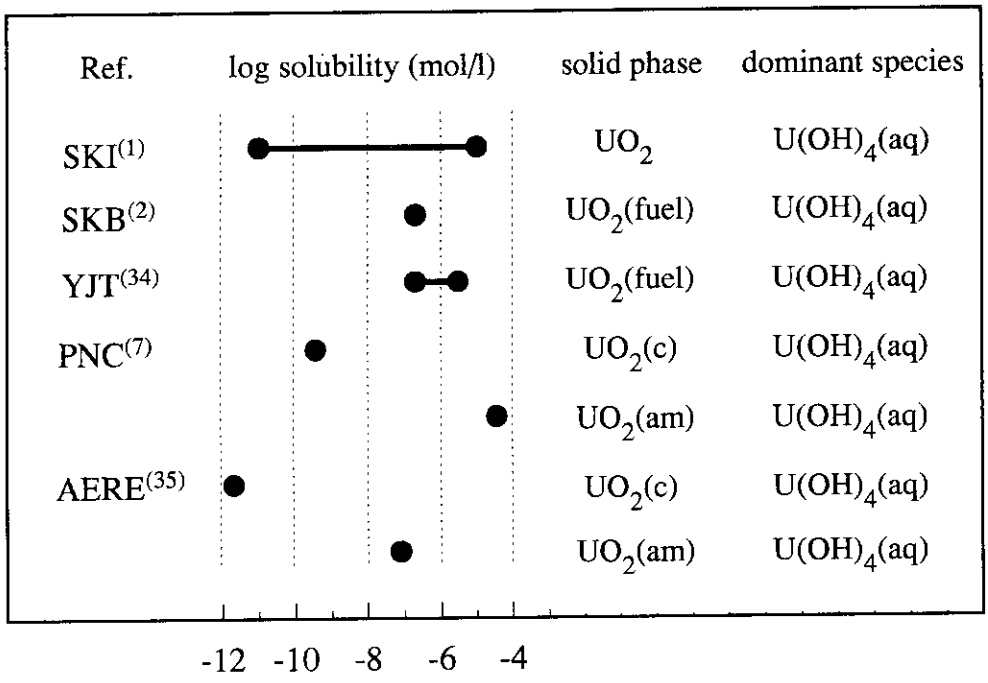

Table 6b Literature data on soubility and speciation of uranium under oxidizing conditions

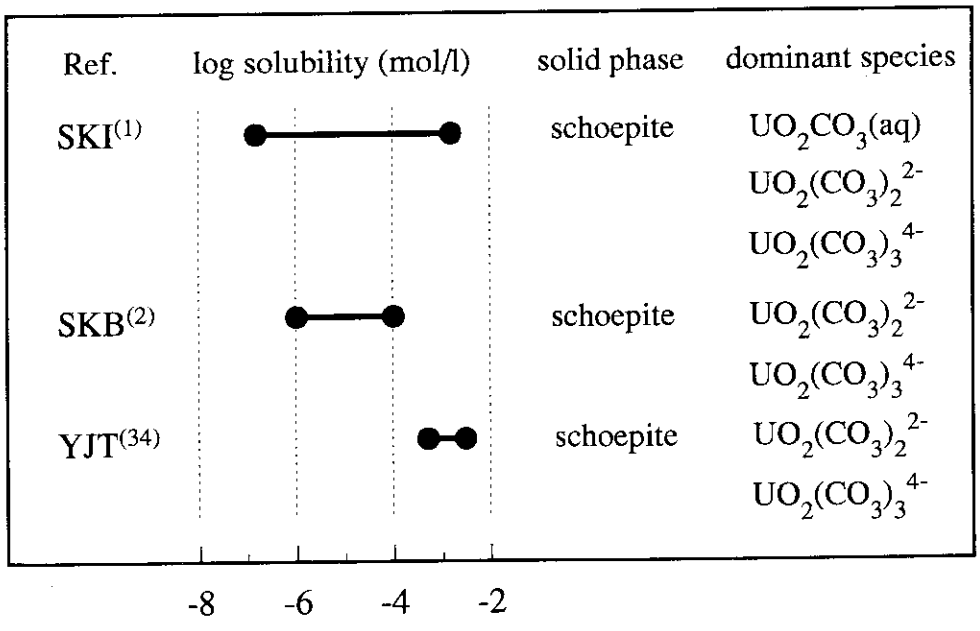

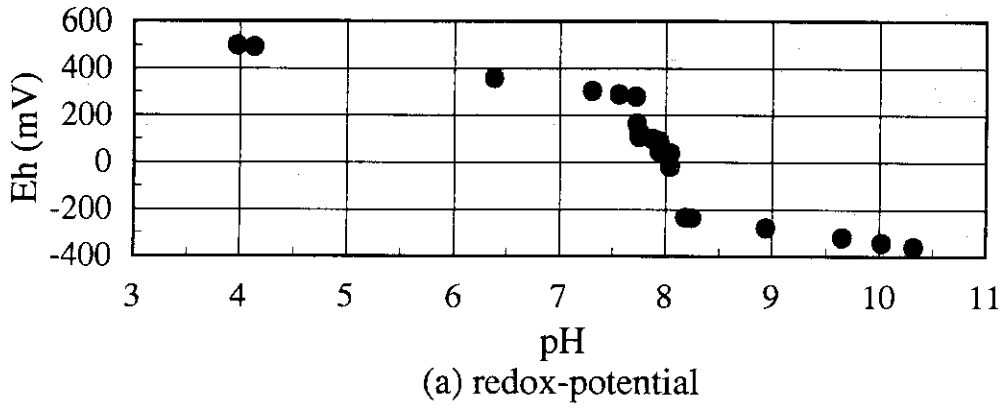

(a) redox-potential

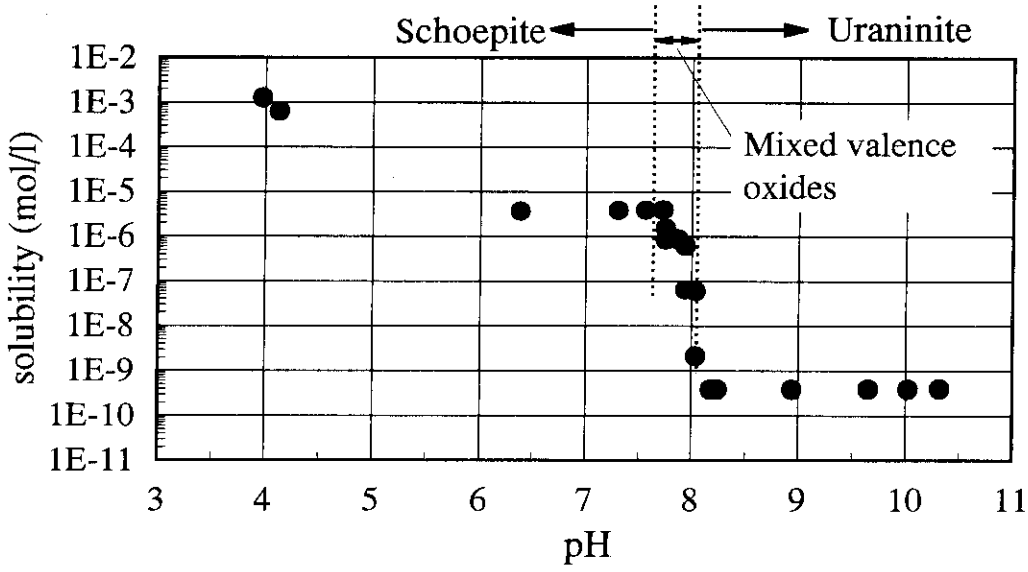

(b) solubility

Fig. 13 Solubility of uranium in the natural barrier

Mixed valence oxides: $U_4O_9(c) \rightarrow U_3O_7(c, \beta) \rightarrow U_3O_8(c)$

(oxidizing environments: $4<pH<8$, $5 \cdot 10^{-14} < [CO_3^{2-}] < 10^{-6}$ mol/l)

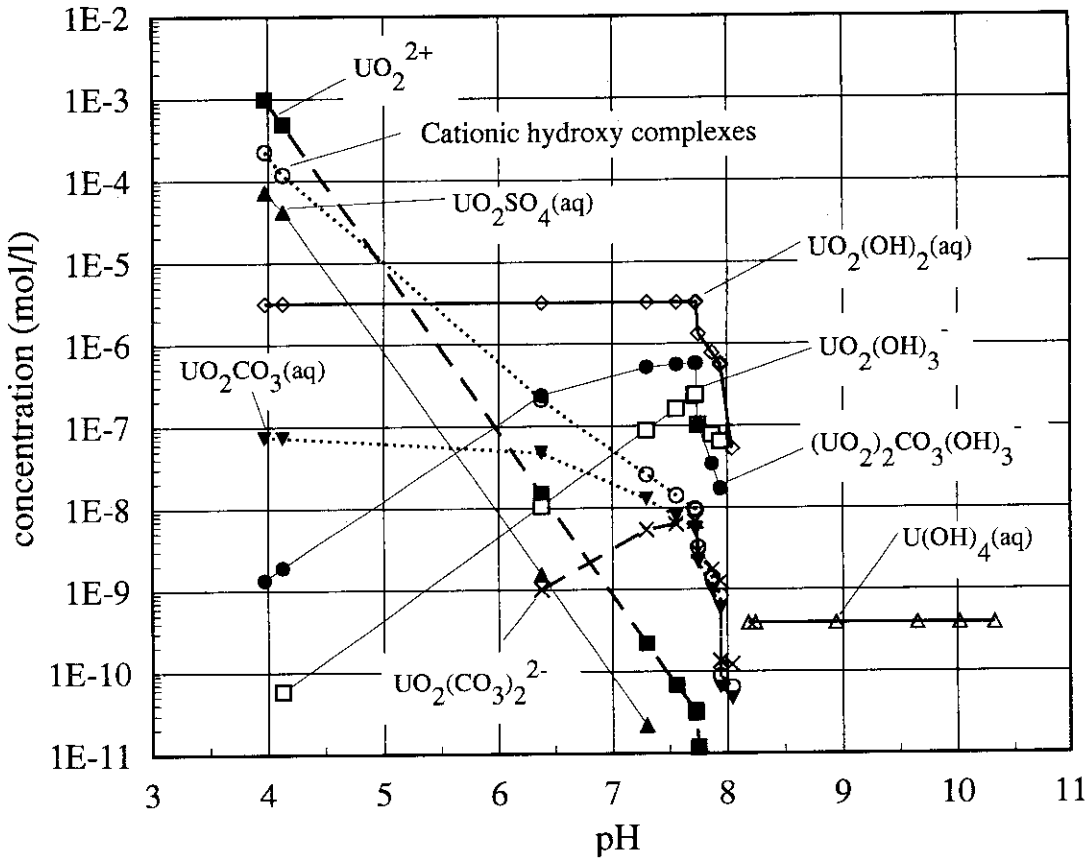

Fig. 14 Speciation of uranium in the natural barriers. Cationic hydroxy complexes; UO_2OH^+, $(UO_2)_2OH^{3+}$, $(UO_2)_2(OH)_2^{2+}$, $(UO_2)_3(OH)_4^{2+}$, $(UO_2)_3(OH)_5^+$, $(UO_2)_4(OH)_7^+$ (oxidizing environments: $4<pH<8$, $5\times10^{-14}< [CO_3^{2-}] < 10^{-6}$ mol/l)

dominant aqueous species is hydroxy complexes of U(IV). The abundance of $U(OH)_5^-$ is only 3 % at pH 10.3, and then the dominant species of uranium in the engineered barrier might be neutral $U(OH)_4(aq)$. Under the reducing conditions, the comparison of data on the solubility and speciation for U reported in the literatures referred here is shown in Table 5a. Dominant aqueous species of this analysis is identical with all of the reviewed analyses. The range of the solubility of uranium in Table 6a is from 10^{-12} to 10^{-4} mol/l. The solubility of UO_2(c) of PNC[7] is higher in two orders of magnitude than that of AERE[34], and the difference of solubility of UO_2(am) between PNC and AERE is in about three orders of magnitude. It is inferred that the thermodynamic data of UO_2(c) and UO_2(am) used in PNC and AERE are different. As mentioned in section 2.5., it is predicted that the solubility of amorphous UO_2 is higher than that of UO_2(c). Viewed in the radiological importance of uranium in safety assessment, further critical examination of its thermodynamic data should be conducted to prepare a more precise data set to be used in the calculation.

The range of solubilities of uranium obtained by Model 2 is shown in Fig. 13. In the engineered barrier, the solubility increases with increasing the redox potential, i.e., with changing

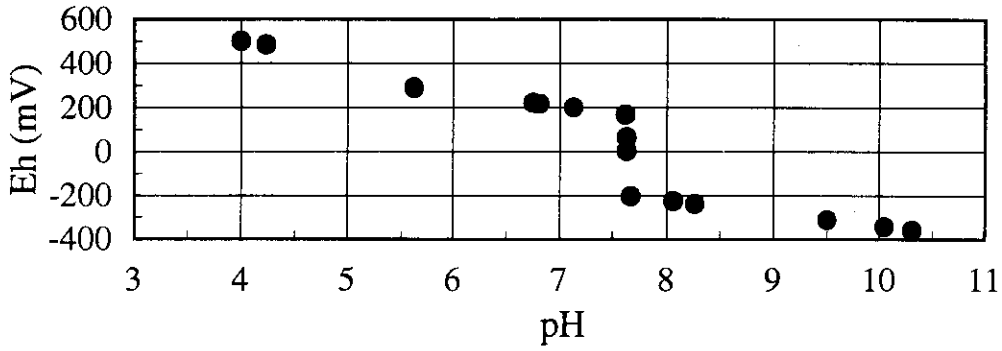

(a) redox-potential

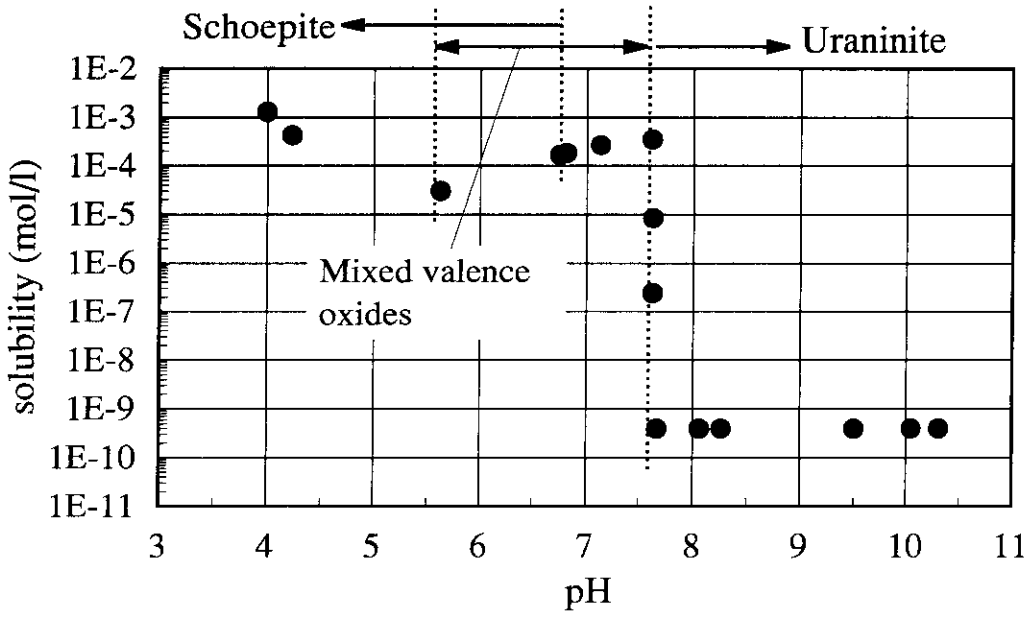

(b) solubility

Fig. 15 Solubility of uranium in the natural barrier
Mixed valence oxides: $U_4O_9(c) \rightarrow U_3O_7(c, \beta) \rightarrow U_3O_8(c)$
(oxidizing environments: $4<pH<7.6$, $5\times10^{-12}< [CO_3^{2-}] < 10^{-5}$ mol/l)

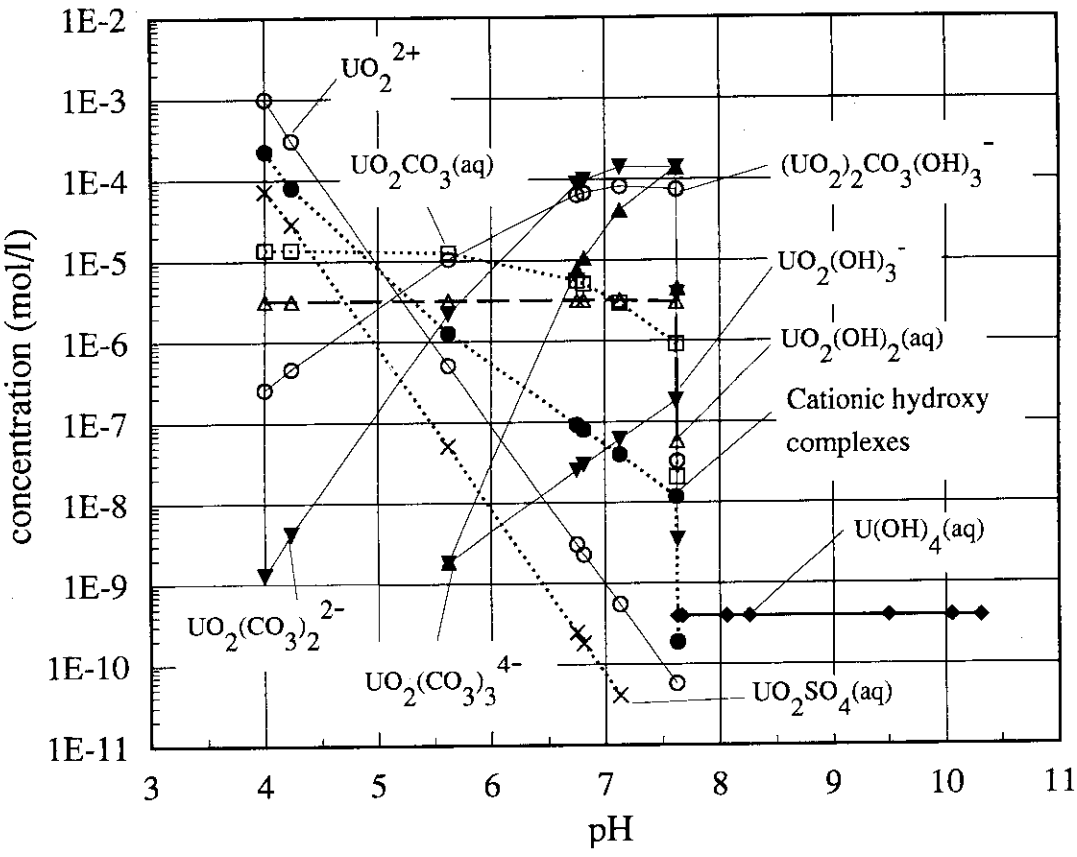

Fig. 16 Speciation of uranium in the natural barriers. Cationic hydroxy complexes; UO_2OH^+, $(UO_2)_2OH^{3+}$, $(UO_2)_2(OH)_2^{2+}$, $(UO_2)_3(OH)_4^{2+}$, $(UO_2)_3(OH)_5^+$, $(UO_2)_4(OH)_7^+$ (oxidizing environments, 4<pH<7.6, $5\times10^{-12} < [CO_3^{2-}] < 10^{-5}$ mol/l)

of the electrochemical conditions from the reducing to the oxidizing environments. In the reducing environment in which uraninite is stable, the solubility remains constant, but increases up to 6×10^{-8} mol/l while the solid phase changes into U_4O_9(c). Further increase of the solubility is observed, owing to that the solid phase changes from U_3O_7(c, β) to U_3O_8(c). At more oxidizing conditions, the solid phase of U is in equilibrium with schoepite and the corresponding solubility amounts to 4×10^{-6} mol/l at Eh 280 mV and pH 7.7. In the oxidizing groundwater in the surface layer, the solubility of uranium further increases up to about 10^{-3} mol/l. With an increase of Eh and also a decrease of pH, the oxidation state varies from tetravalent to hexavalent, and the stable solid phase of uranium for Model 2 exhibits the following sequence; uraninite → U_4O_9(c) → U_3O_7(c, β) → U_3O_8(c) → schoepite. The change in the aqueous species of uranium obtained by Model 2 is shown in Fig. 14. The dominant aqueous species, $U(OH)_4$(aq), changes into hydroxy or carbonate complexes of U(VI) at pH 8. The neutral $UO_2(OH)_2$(aq) species is the most dominant in the oxidizing groundwater in the pH region of 8 to 5.5. Carbonate complexes, UO_2CO_3(aq), $UO_2(CO_3)_2^{2-}$, and $(UO_2)_2CO_3(OH)_3^-$ exist in the groundwater, and the total maximum abundance of

them amounts to about 15 %. The concentration of CO_3^{2-} changes from $5x10^{-14}$ to 10^{-6} mol/l at the conditions of pH range from 4 to 8 and the total carbonate concentration of $2.3x10^{-5}$ mol/l. Uranyl ion, UO_2^{2+}, and six uranium hydroxy complexes in hexavalent state are stable in the oxidizing environments below pH 5.5. All of these species have positive charges. Also, sulfate complex $UO_2SO_4(aq)$ exists in the oxidizing groundwater at the ratio of 15 % .

The concentration of CO_3^{2-} will influence the solubility and speciation of uranium under the oxidizing conditions. Another analysis by Model 2 was performed under the condition of a higher carbonate concentration in the oxidizing groundwater. The total carbonate concentration was set as $4.4x10^{-3}$ mol/l being higher in about two orders of magnitude than that used in the analysis mentioned above. The range of CO_3^{2-} concentration is from $5x10^{-12}$ to 10^{-5} mol/l in the pH region of 4 to 7.6. The change of the solubility for this case is shown in Fig. 15. The stable solid phase analyzed by the reaction path model varies as follows; uraninite $\rightarrow U_4O_9(c) \rightarrow U_3O_7(c, \beta) \rightarrow U_3O_8$ (c)$\rightarrow$ schoepite. While uraninite changes into $U_4O_9(c)$ or $U_3O_7(c, \beta)$, the solubility of uranium increases up to $4x10^{-4}$ mol/l. This value is higher about two orders of magnitude than that obtained with the lower carbonate concentration ($2.3x10^{-5}$mol/l). After that, the solubility decreases with increasing Eh and decreasing pH, but again increases in the pH region below 5.5. The speciation of uranium in the natural groundwater is shown in Fig. 16. Carbonate complexes of $UO_2(CO_3)_2^{2-}$, $UO_2(CO_3)_3^{4-}$, and $(UO_2)_2CO_3(OH)_3^-$ predominate in the oxidizing groundwater. The concentrations of these uranium carbonate complexes decrease in the pH region below 7.6 due to the decrease of CO_3^{2-} concentration with a lowering of pH. The change of uranium solubility in the pH region from 7.6 to 6 is controlled by the concentrations of the carbonate complexes mentioned above. A higher solubility of uranium in neutral pH range resulted from the increase in the concentrations of these carbonate complexes. The solubility of uranium, however, does not depend on the CO_3^{2-} concentration in the pH region below 5, where the concentrations of carbonate ions are too low to form U carbonates. The comparison of literature data on the uranium solubility and speciation, under the oxidizing conditions, is shown in Table 6b. The pH range in the reports referred in Table 6b is from neutral to alkaline, and the Eh-pH conditions used in this study are different from these conditions reported. The range of the solubility obtained here by assuming the equilibrium with schoepite, from 10^{-5} to 10^{-3} mol/l, shows excellent agreement with the reported range, from 10^{-7} to $3x10^{-3}$ mol/l. The stable aqueous species are carbonate complexes of U(VI) in all literatures cited here, and this is in agreement with the analyzed results obtained here for the neutral pH region.

3.2 Neptunium

Under the reducing conditions, the solubility and speciation of neptunium in Model 1 are shown in Fig. 17. The solubility of the assumed solubility limiting solid phase, $Np(OH)_4(s)$, remains constant at $8x10^{-9}$ mol/l, and is not influenced by the change of the composition of interstitial water involved in the engineered barrier. The dependence of neptunium solubility on

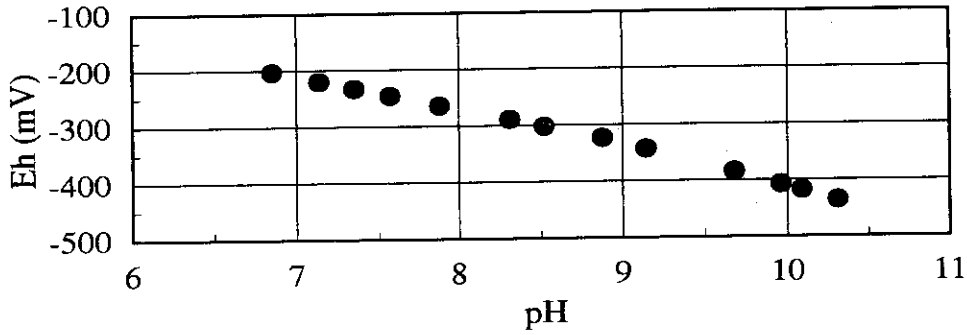

(a). redox-potential

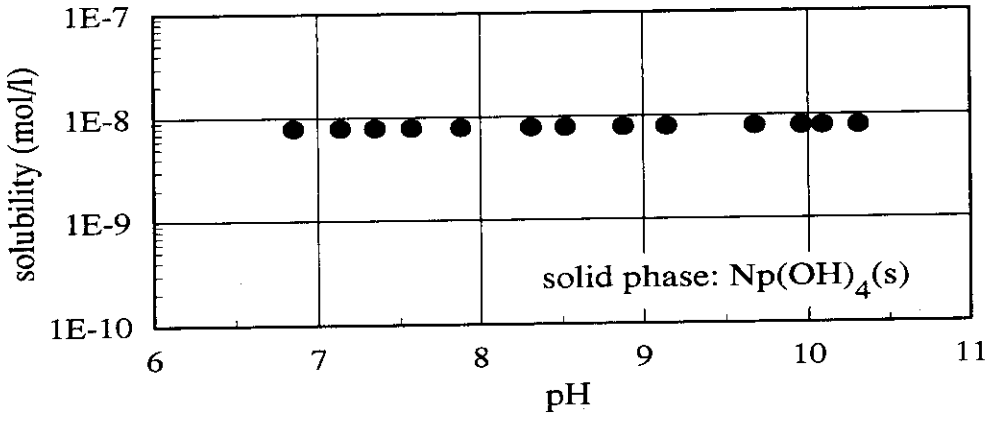

(b). solubility

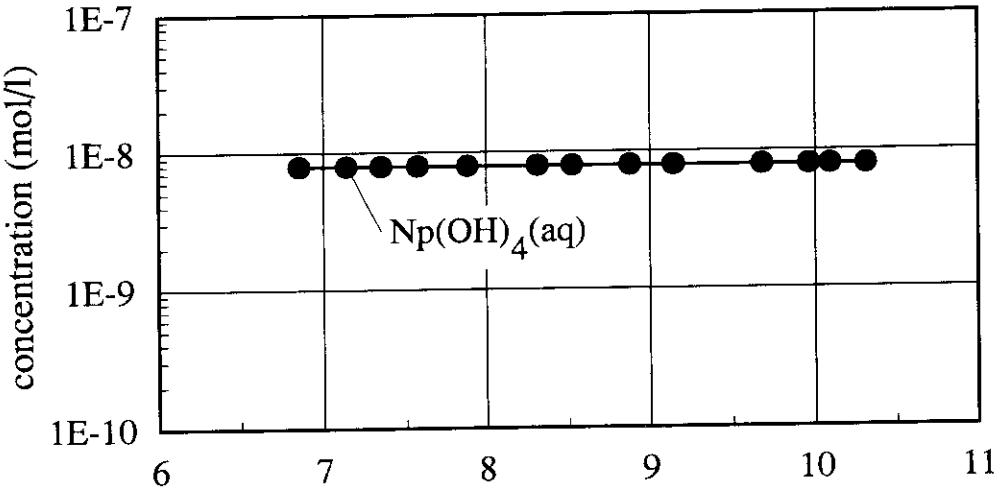

(c). speciation

Fig. 17 Solubility and speciation of neptunium in the engineered barrier (reducing environments)

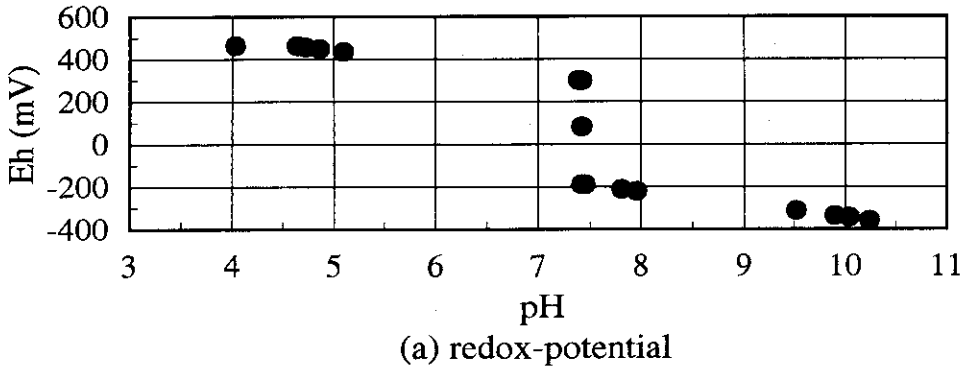

(a) redox-potential

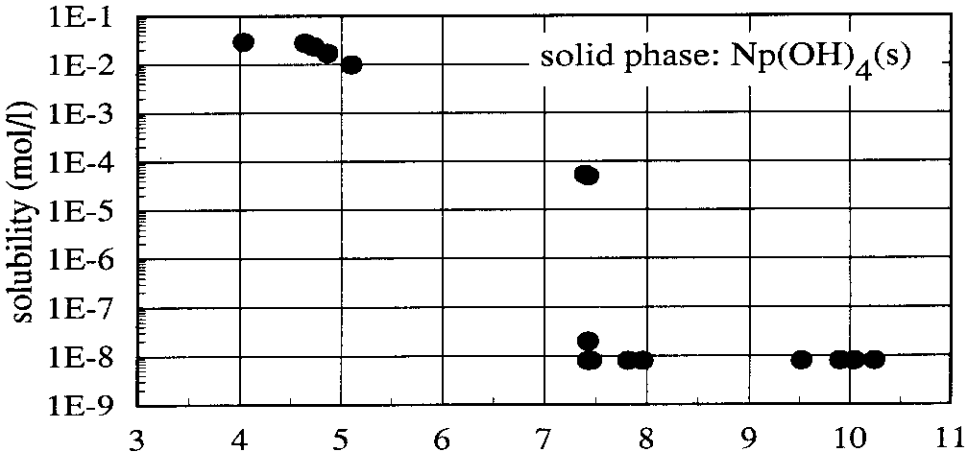

(b) solubility

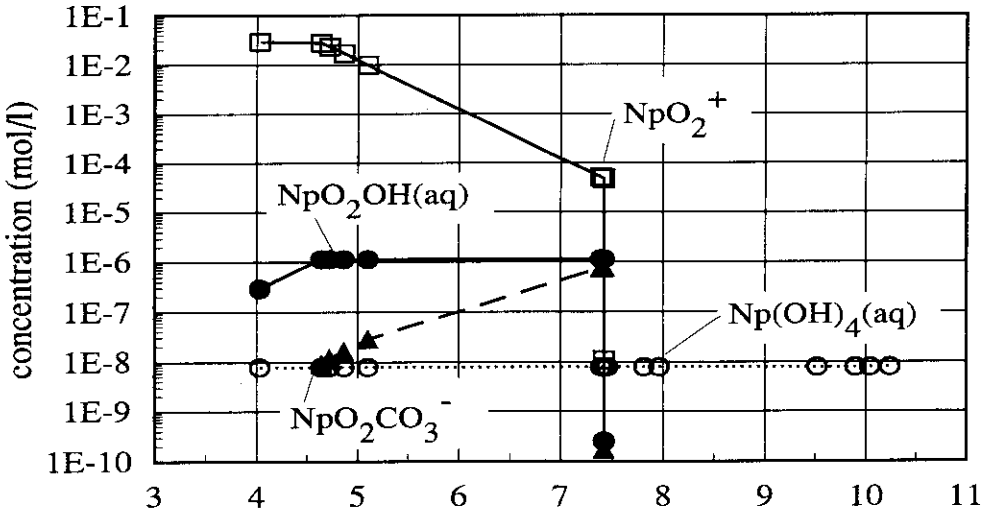

(c) speciation

Fig. 18 Solubility and speciation of neptunium in the natural barrier
(oxidizing environments: 4<pH<7.4, $5\times10^{-14} < [CO_3^{2-}] < 4\times10^{-6}$ mol/l)

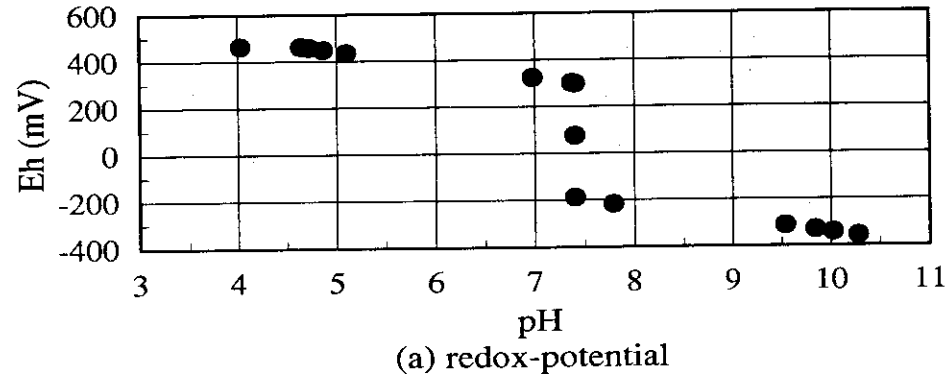

(a) redox-potential

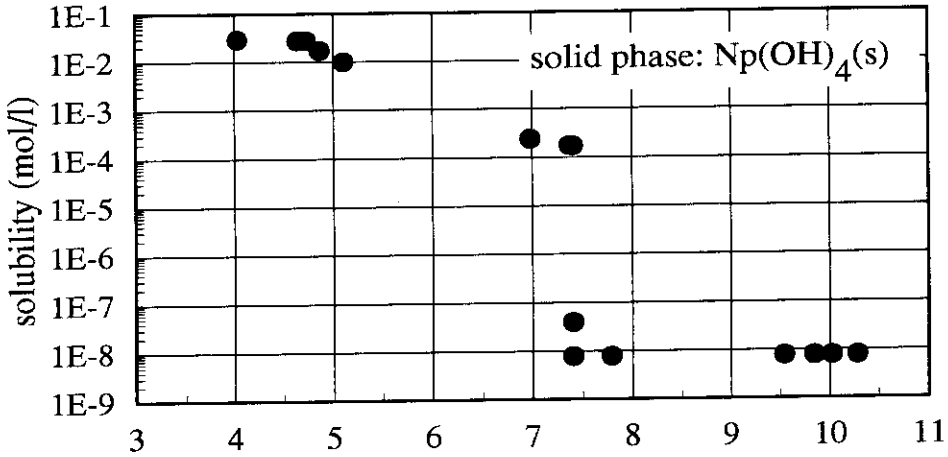

(b) solubility

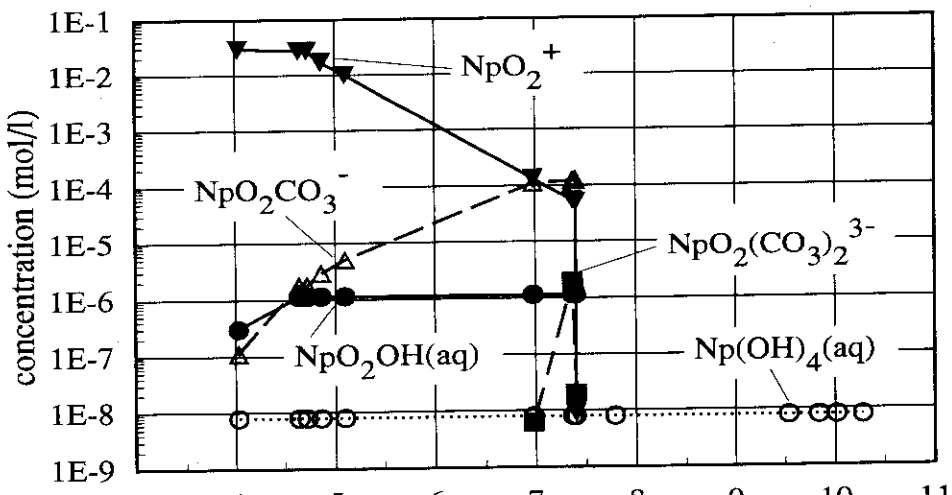

(c) speciation

Fig. 19 Solubility and speciation of neptunium in the natural barrier
(oxidizing environments: 4<pH<7.4, 8×10^{-12}< [CO_3^{2-}] < 6×10^{-6} mol/l)

Table 7a Literature data on soubility and speciation of neptunium under reducing conditions

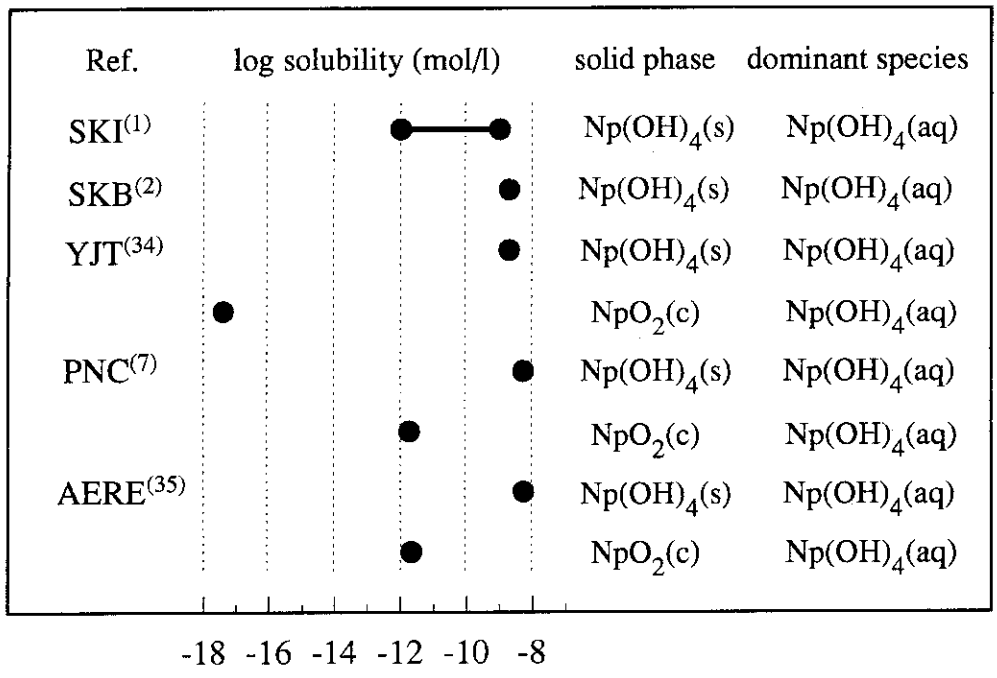

Table 7b Literature data on soubility and speciation of neptunium under oxidizing conditions

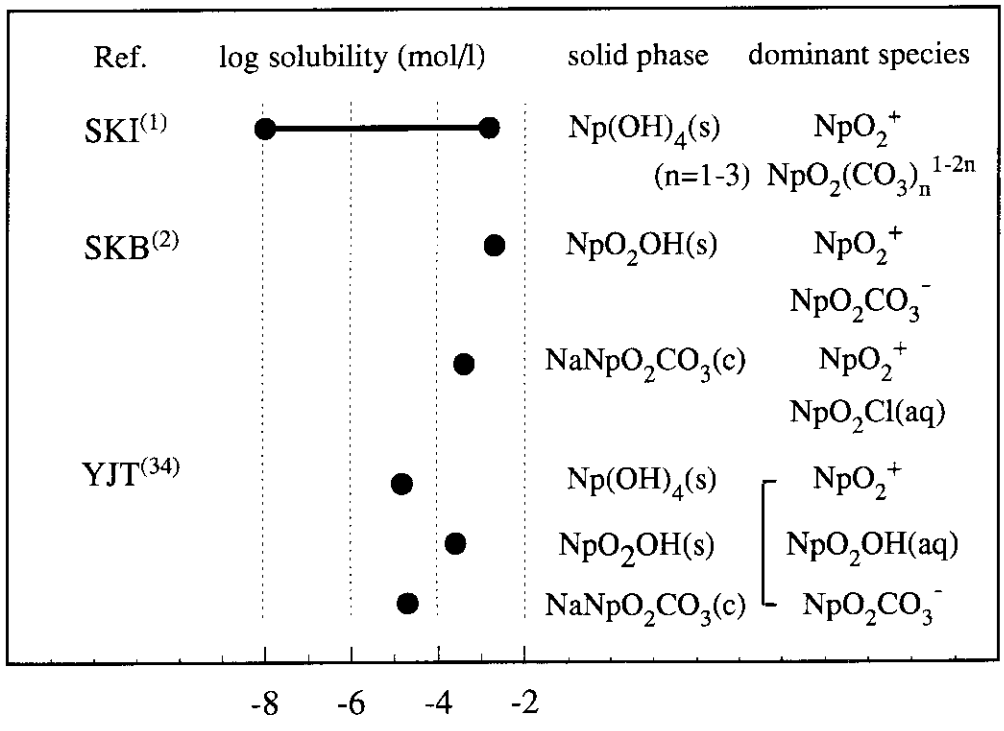

the geochemical conditions in the reducing environments is similar to that of uranium. The Np (IV) aqueous species is dominated by the neutral hydroxy complex, $Np(OH)_4(aq)$. Literature data on the solubility and speciation of neptunium under the reducing conditions are shown in Table 7a. The calculated solubility and speciation seem to be in good agreement with those reported by the literatures. As seen from Table 6a, the solubility of $NpO_2(c)$ distributes from 10^{-18} to 10^{-11}mol/l, probably owing to a large uncertainty being included in the thermodynamic data used in the literatures referred here.

In Model 2 under the oxidizing conditions, the total carbonate concentrations of the groundwater in the natural barrier were set as two cases, $2.3x10^{-5}$ and $4.4x10^{-3}$ mol/l, in order to clarify the effect of CO_3^{2-} concentration on the solubility and speciation of neptunium. The results of analysis on the solubility and aqueous speciation are given in Fig. 18. The CO_3^{2-} concentration varies from $5x10^{-14}$ to $4x10^{-6}$ mol/l in the pH range of 4 to 7.4. When the redox-potential shifts from -200 to 300 mV at pH 7.4, the dominant aqueous species changes from $Np(OH)_4(aq)$ into a hydroxide of Np(V). The solubility of neptunium in equilibrium with $Np(OH)_4(s)$ increases up to $5x10^{-5}$ mol/l owing to the change of redox-potential. Below pH 7.4, the solubility of $Np(OH)_4(s)$ shows an increasing tendency, and finally increases up to $3x10^{-2}$ mol/l at Eh 500 mV. Under the oxidizing conditions, the predominant aqueous species of neptunium is the cationic neptunyl ion NpO_2^+. Hydroxy and carbonate complexes of $NpO_2OH(aq)$ and $NpO_2CO_3^-$ in a few percentages exist in the oxidizing groundwater.

The results analyzed by Model 2 at the carbonate concentration of $4.4x10^{-3}$ mol/l are shown in Fig. 19. The CO_3^{2-} concentrations range from $8x10^{-12}$ to $6x10^{-6}$ mol/l at the pH between 4 and 7.4. There was no difference in the tendency in varying solubilities which were calculated under two types of the carbonate concentrations. The abundance of $NpO_2CO_3^-$, which is predominant only in the pH region of 7 to 7.4, is larger for this case than that for the lower carbonate concentration ($2.3x10^{-5}$ mol/l). It might be said that in the oxidizing environments the carbonate complexes of Np(V) can not be predominant under the conditions; total carbonate concentration of $4.4x10^{-3}$mol/l and pH<7. Under the oxidizing conditions, the comparison of the solubility and speciation of neptunium reported in the literatures is shown in Table 7b. The result calculated here of the solubility is similar to that of SKI. The result obtained in this study, where the dominant aqueous species are both NpO_2^+ and $NpO_2CO_3^-$, is almost identical with those of the literatures referred here, but other carbonate complexes of Np(V), $NpO_2OH(aq)$, and $NpO_2Cl(aq)$ are also reported as one of the dominant aqueous species of Np(V) under the oxidizing environments.

3.3 Selenium

The results of selenium analyzed by Model 1 in the engineered barrier are shown in Fig. 20. The pH dependence of the solubilities for two solubility limiting solid phases, Se(c) and $FeSe_2(c)$, is shown in Fig. 20(b). Both of the solubilities tend to rise with increasing pH and decreasing Eh. The solubility of Se(c) is higher in two orders of magnitude than that of $FeSe_2(c)$. The solubility of

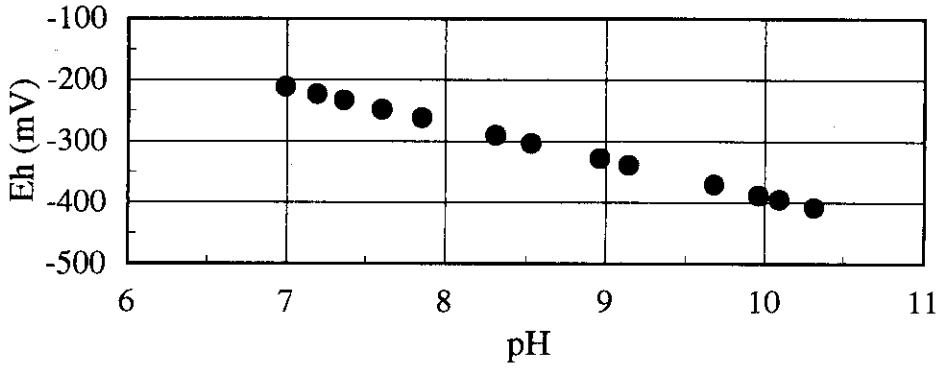

(a) redox-potential

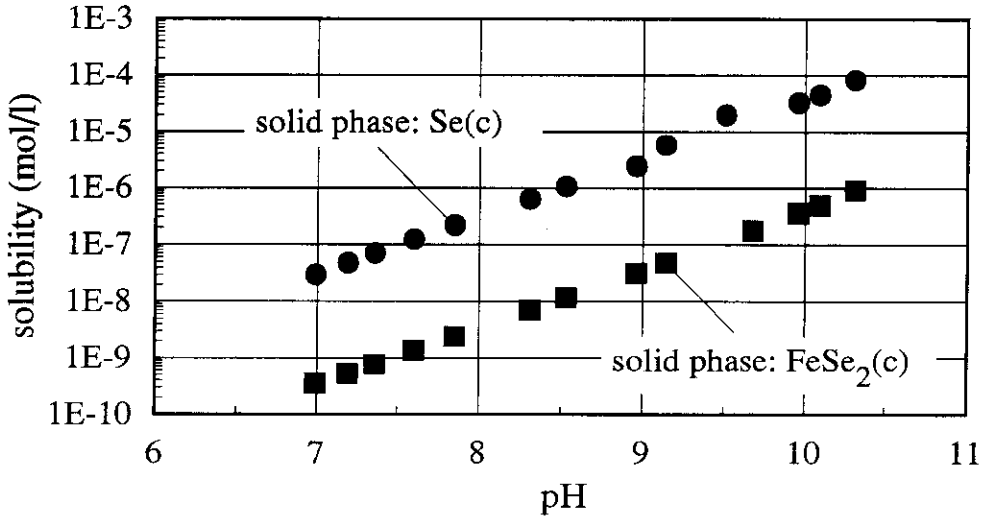

(b) solubility

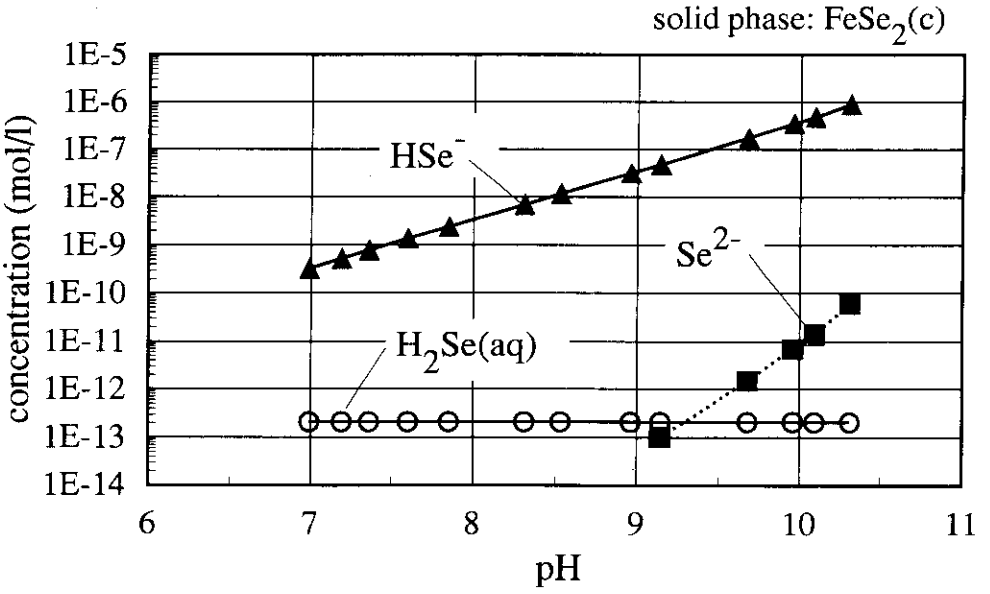

(c) speciation

Fig. 20 Solubility and speciation of selenum in the engineered barrier (reducing environments)

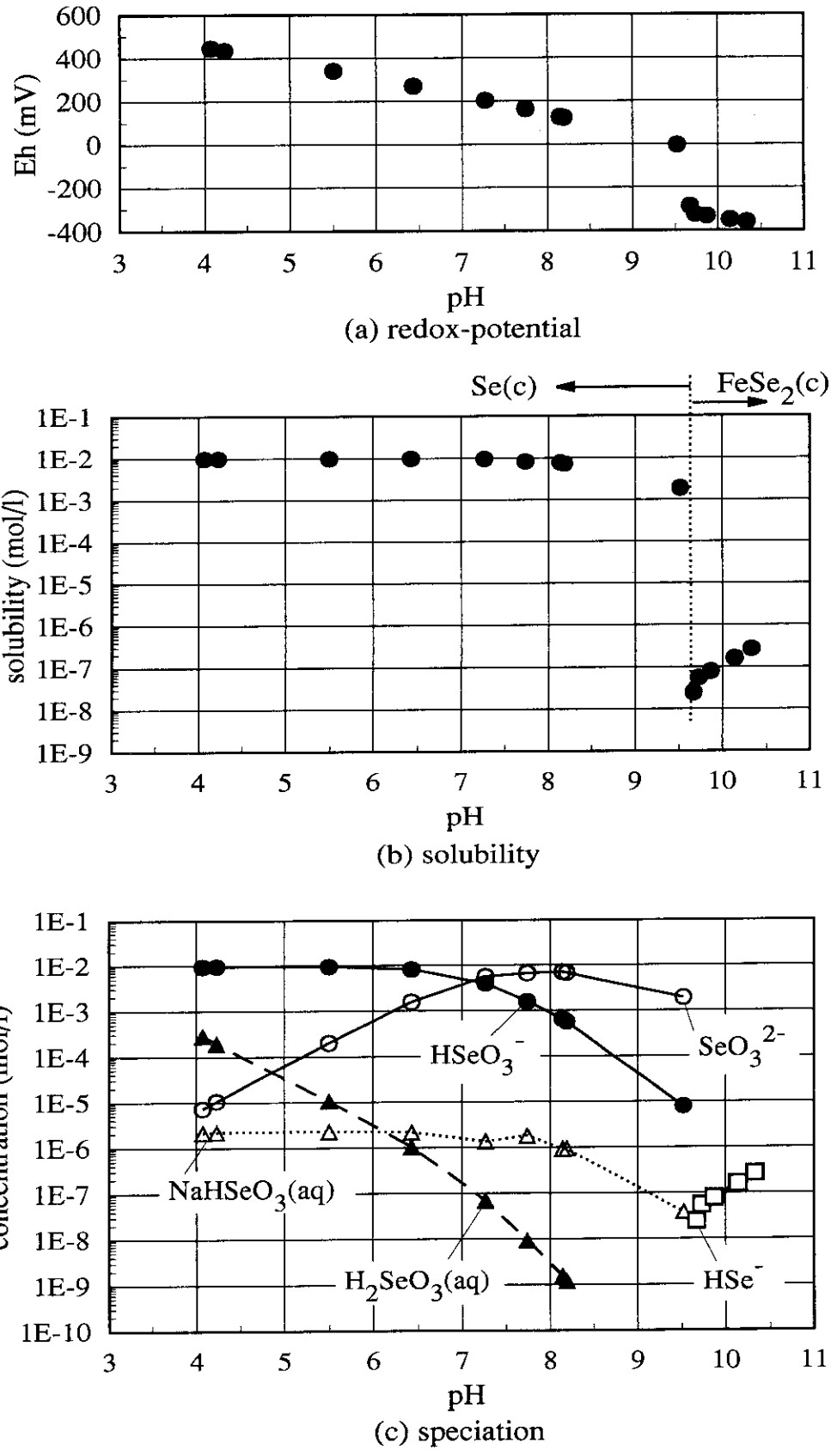

Fig. 21 Solubility and speciation of selenum in the natural barrier (oxidizing environments)

Table 8a Literature data on soubility and speciation of selenium under reducing condition

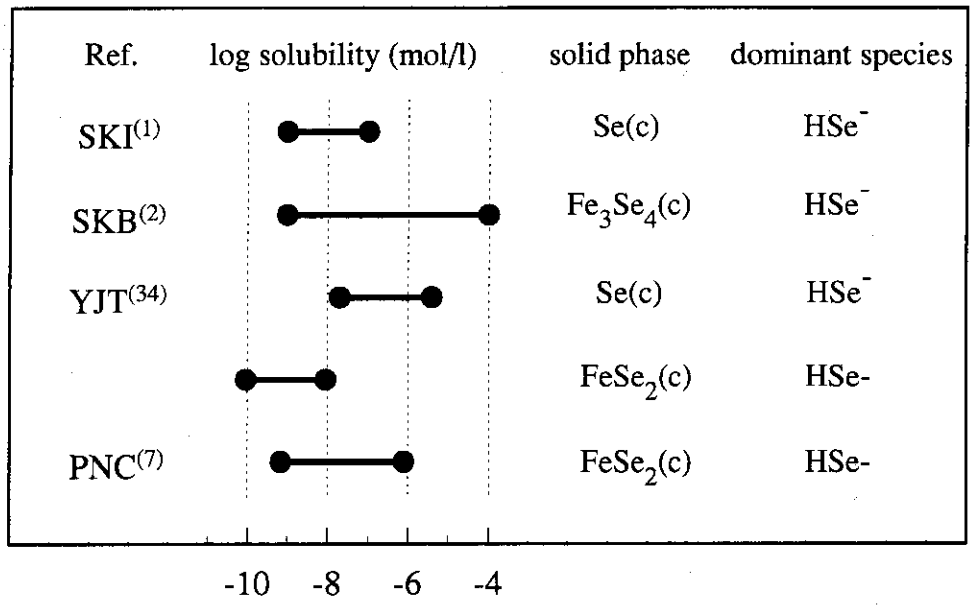

Table 8b Literature data on soubility and speciation of selenium under oxidizing conditions

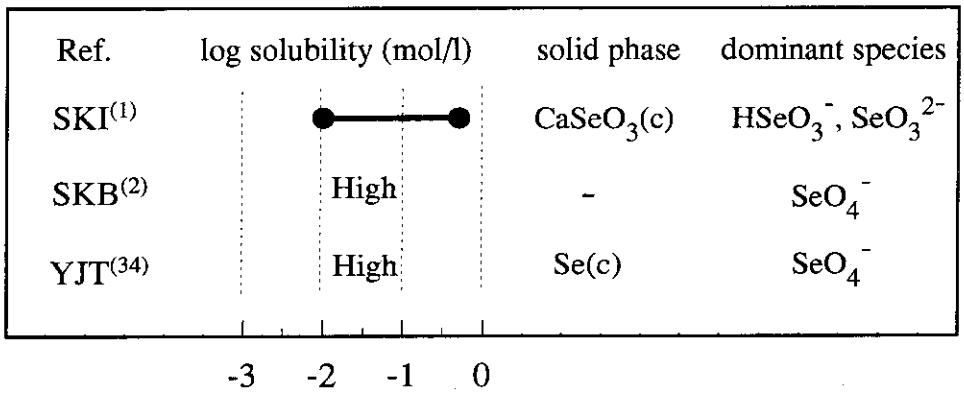

Se(c), which was assumed as the solubility limiting solid phase, increases up to 8.4×10^{-5} mol/l under the condition; pH 10.3 and Eh -410mV. The pH dependence of the concentrations of the aqueous species, HSe^-, $H_2Se(aq)$ and Se^{2-}, in equilibrium with $FeSe_2(c)$ is shown in Fig. 20(c). The aqueous species of selenide(-II) are stable in the reducing environments. The existence of Se^{2-} and $H_2Se(aq)$ is confirmed in the pH range of neutral to alkaline, but their abundances are extremely low. In the engineered barrier the stable aqueous species is HSe^- with negative charge under the reducing conditions. Table 8a shows that the dominant aqueous species of Se is identical among the literatures referred here and this analysis. The calculated solubility range of $FeSe_2(c)$ is almost identical with that of PNC. The calculated solubility range of Se(c), from 3×10^{-8} to 8×10^{-5} mol/l, is higher in one order of magnitude than that of YJT, which reports the highest solubility range of Se(c). The highest solubility obtained here was calculated at pH 10.3

and Eh -410mV, while that of YJT at pH 8.9 and Eh -300mV. The caluculated solubility of Se(c) is higher than that of YJT because the solubility of Se(c) tends to rise with increasing pH and decreasing Eh. The solubility limiting solid phase is assumed to be Fe_3Se_4(c) in SKB report, and the solubility range of its solid phase tends to be higher than other solubility ranges. It is considered that the thermodynamic stability of Fe_3Se_4(c) is lower than that of $FeSe_2$(c) in the reducing environments, however, that the solubility and the thermodynamic stability of Fe_3Se_4(c) must be subjected to a critical examination because the solubility of Fe_3Se_4(c) reported in SKB is higher.

In the natural barrier, the analyzed results of selenium for Model 2 is shown in Fig. 21. The solid phase, $FeSe_2$(c), which is stable in the reducing environments, changes into Se(c) in the oxidizing environments. The solubility in equilibrium with Se(c) sharply increases up to $2x10^{-3}$ mol/l at pH 9.7 and Eh 0.0 mV. The solubility under this condition is higher in five orders of magnitude than that under the reducing conditions. In the neutral and alkaline pH ranges, the solubility remains constant at 10^{-2} mol/l. In the natural barrier, the selenium solubility tends to be very high under the oxidizing conditions. The aqueous species of selenium changes from selenide (-II) to selenite(IV) with the increase of the redox-potential in the natural barrier. Under the oxidizing conditions, the predominant aqueous species is SeO_3^{2-} in the pH range of 9.7 to 7.3, and changes into $HSeO_3^-$ below pH 7.3. It is inferred that such anions as SeO_3^{2-} and $HSeO_3^-$ predominate in the natural groundwater under the oxidizing environments. Also a very small amount of $NaSeO_3$(aq) exists in the oxidizing groundwater. The solubility of $NaSeO_3$(aq) is too high to be negligible in the oxidizing groundwater including NaCl of high concentration. The literature data on solubility and speciation of selenium under the oxidizing conditions are shown in Table 8b. In SKI report, the solubility limiting solid phase of Se under the oxidizing conditions is assumed to be $CaSeO_3$(c), and its solubility range is higher than that of Se(c) obtained in this study. The high solubility of Se in the oxidizing environment is also reported by SKB and YJT.

4. CONCLUSION

Solubility, the aqueous species, and the stable solid phase for elements provide scientific bases for safety assessment of geologic disposal of HLW and depend on chemical characteristics of groundwater such as composition, ionic strength, Eh-pH condition. For example, the distribution coefficient which is widely used in safety assessment of radioactive waste disposal, is influenced by the stable aqueous species of each element in a specific geological environment. In this study, the solubility and speciation analyses for uranium, neptunium, and selenium in a disposal system were performed by using the geochemical code EQ3/6. Taking account of the space- and time-varying chemical conditions of the groundwater, two kinds of groundwater models were assumed based on the measured compositions; Model 1 simulates the composition of

and Eh -410mV, while that of YJT at pH 8.9 and Eh -300mV. The caluculated solubility of Se(c) is higher than that of YJT because the solubility of Se(c) tends to rise with increasing pH and decreasing Eh. The solubility limiting solid phase is assumed to be Fe_3Se_4(c) in SKB report, and the solubility range of its solid phase tends to be higher than other solubility ranges. It is considered that the thermodynamic stability of Fe_3Se_4(c) is lower than that of $FeSe_2$(c) in the reducing environments, however, that the solubility and the thermodynamic stability of Fe_3Se_4(c) must be subjected to a critical examination because the solubility of Fe_3Se_4(c) reported in SKB is higher.

In the natural barrier, the analyzed results of selenium for Model 2 is shown in Fig. 21. The solid phase, $FeSe_2$(c), which is stable in the reducing environments, changes into Se(c) in the oxidizing environments. The solubility in equilibrium with Se(c) sharply increases up to $2x10^{-3}$ mol/l at pH 9.7 and Eh 0.0 mV. The solubility under this condition is higher in five orders of magnitude than that under the reducing conditions. In the neutral and alkaline pH ranges, the solubility remains constant at 10^{-2} mol/l. In the natural barrier, the selenium solubility tends to be very high under the oxidizing conditions. The aqueous species of selenium changes from selenide (-II) to selenite(IV) with the increase of the redox-potential in the natural barrier. Under the oxidizing conditions, the predominant aqueous species is SeO_3^{2-} in the pH range of 9.7 to 7.3, and changes into $HSeO_3^-$ below pH 7.3. It is inferred that such anions as SeO_3^{2-} and $HSeO_3^-$ predominate in the natural groundwater under the oxidizing environments. Also a very small amount of $NaSeO_3$(aq) exists in the oxidizing groundwater. The solubility of $NaSeO_3$(aq) is too high to be negligible in the oxidizing groundwater including NaCl of high concentration. The literature data on solubility and speciation of selenium under the oxidizing conditions are shown in Table 8b. In SKI report, the solubility limiting solid phase of Se under the oxidizing conditions is assumed to be $CaSeO_3$(c), and its solubility range is higher than that of Se(c) obtained in this study. The high solubility of Se in the oxidizing environment is also reported by SKB and YJT.

4. CONCLUSION

Solubility, the aqueous species, and the stable solid phase for elements provide scientific bases for safety assessment of geologic disposal of HLW and depend on chemical characteristics of groundwater such as composition, ionic strength, Eh-pH condition. For example, the distribution coefficient which is widely used in safety assessment of radioactive waste disposal, is influenced by the stable aqueous species of each element in a specific geological environment. In this study, the solubility and speciation analyses for uranium, neptunium, and selenium in a disposal system were performed by using the geochemical code EQ3/6. Taking account of the space- and time-varying chemical conditions of the groundwater, two kinds of groundwater models were assumed based on the measured compositions; Model 1 simulates the composition of

the interstitial water in the engineered barrier, and Model 2 is the composition of the granitic groundwater in the natural barrier.

4.1 Solubility and Speciation in the Engineered Barrier

The analyzed results of solubility and speciation under the reducing conditions in the engineered barrier are summarized in Table 9. The following remarks are derived through solubility and speciation analyses of uranium, neptunium, and selenium by Model 1.

(1) In the engineered barrier, the solubility in equilibrium with uraninite (UO_2(c)) is not influenced by the change in the chemical composition of the interstitial water, and remains constant at $4x10^{-10}$ mol/l. The solubility of amorphous UO_2 is markedly higher than that of uraninite. From a viewpoint of safety assessment, it is of importance to predict the solubility of amorphous UO_2. The precise thermodynamic data even for uranium might be far from to be established , and further critical review of the data must be carried out. The predominant aqueous species is uranium hydroxy complex in tetravalent state, $U(OH)_4$(aq). It might be said that $U(OH)_4$(aq) with neutral charge leads to low sorption on the buffer materials having negative charges on the surface.

(2) In the engineered barrier, the solubility and speciation of neptunium are similar to those of uranium under the reducing conditions. The solubility of $Np(OH)_4$(s), which was assumed to be the solubility limiting solid phase, is constant at $8x10^{-9}$ mol/l under the Eh-pH conditions ; 6.8<pH<10.3 and -200<Eh<-435mV. The solubility of NpO_2(c) might be lower than that of $Np(OH)_4$(s), and its calculated solubility range distributes widely, probably owing to a large uncertainty involved in the thermodynamic data of NpO_2(c). Under the reducing conditions, the predominant aqueous species is $Np(OH)_4$(aq) with no charge. The sorption of such neutral species on the buffer materials might be of insignificance under the reducing conditions, taking account of a poor electrostatic interaction between them.

(3) The solubility of Se(c) is higher in about two orders of magnitude than that of $FeSe_2$(c). The solubility in equilibrium with Se(c) increases from $3x10^{-8}$ to $8x10^{-5}$ mol/l with the change of Eh-pH condition, i.e., with decreasing Eh and increasing pH , in the reducing environments. The predominant aqueous species is selenide, HSe^-, under the reducing conditions. It might be indicated that HSe^- with negative charge is little retained by the buffer materials.

4.2 Solubility and Speciation in the Natural Barrier

The chemical behaviors of uranium and neptunium might depend on the carbonate concentration in the oxidizing groundwater. The solubility and speciation analyses by Model 2 in the natural barrier were performed under two kinds of the carbonate concentrations. In the natural barrier, the analyzed results by Model 2 are summarized in Table 10. The remarks on the solubility and speciation for U, Np, and Se obtained from these results are as follows;

(1) Tow kinds of the total carbonate concentrations for Model 2 were assumed as follows;

$2.3x10^{-5}$ mol/l (termed as Model 2A hereinafter), $4.4x10^{-3}$ mol/l (termed as Model 2B hereinafter). The solubilities obtained by the two models tend to increase under the oxidizing conditions. In the pH range of neutral to acidic, the solubility for Model 2A, which was calculated under the higher carbonate concentration, is higher than that for Model 2B. The reason of this might be ascribed to that the solubilities of uranium carbonate complexes in hexavalent state increase with the change of pH from neutral to acidic in the oxidizing environments. The predominant aqueous species of Se changes with such chemical characteristics of aqueous solutions as the Eh-pH condition, the concentrations of co-ions, and so on. While the chemical composition changes from the reducing to oxidizing conditions in the natural barrier, the dominant aqueous species vary as follows; $U(OH)_4(aq) \rightarrow UO_2(OH)_2(aq) \rightarrow UO_2^{2+}$ for Model 2A, and $U(OH)_4(aq) \rightarrow UO_2(CO_3)_n^{2-2n}$ (n=1,3) $\rightarrow UO_2^{2+}$ for Model 2B. With an increase in the redox-potential, the stable solid phase in the natural barrier changes as follows; uraninite $\rightarrow U_4O_9(c) \rightarrow U_3O_7(c, \beta) \rightarrow U_3O_8(c) \rightarrow$ schoepite.

(2) The solubility and speciation analyses of neptunium for Model 2A and Model 2B were performed in the natural barrier. The solubility of neptunium slightly increases with an increase in the carbonate concentration, however, the influence of the carbonate concentration is so small as to be negligible under these Eh-pH conditions. Under the oxidizing conditions, the predominant aqueous species are $NpO_2CO_3^-$ (only in the neutral pH) and mainly neptunyl ion, NpO_2^+, at pH<7. The range in which NpO_2^+ is dominant is wider than the range in which cationic uranium species exist, in the oxidizing environments. The CO_3^{2-} concentration tend to be high in the alkaline oxidizing groundwater. In this case, it might be said that the concentration of the carbonate complexes of Np(IV) can not be ignored under this chemical condition. The most stable solid phase in thermodynamics is $Np(OH)_4(s)$ in the oxidizing environments.

(3) In the natural barrier, the solubility of selenium, which varies from $2x10^{-3}$ to $1x10^{-2}$ mol/l, is very high under the oxidizing conditions. The stable solid phase is Se(c) in the oxidizing environments. While the chemical condition of natural groundwater changes from the reducing to the oxidizing conditions, the predominant aqueous species of Se might exist in the natural barrier as three kinds of anions; $HSe^- \rightarrow SeO_3^{2-} \rightarrow HSeO_3^-$.

(4) As assumed that dominant aqueous species of U, Np, or Se varies during the migration in the natural barrier, such parameters as the distribution coefficient et al. must be determined with considering the dominant aqueous species. For U and Np, the dominant aqueous species with negative or neutral charge might lead to a low sorption under the reducing conditions, and the species with positive charge to high sorption under the oxidizing conditions. Aqueous species of U or Np are dependent on compositions, Eh-pH condition, and carbonate concentration. The prediction for the long-term groundwater compositions is hence indispensable to obtain reliable analytical results

Table 9 Results of solubility and speciation analysis for U, Np and Se in the engineered barrier (reducing conditions)

element	Uranium	Neptunium	Selenium
conditions	Eh : -200 → -435 (mV) pH : 6.8 → 10.3		
solubility (mol/l) solid phase	$4x10^{-10}$ (constant) UO_2(c) (=uraninite)	$8x10^{-9}$ (constant) $Np(OH)_4$(s)	$4x10^{-10} \rightarrow 9x10^{-7}$ $FeSe_2$(c)
			$3x10^{-8} \rightarrow 8x10^{-5}$ Se(c)
dominant species	$U(OH)_4$(aq)	$Np(OH)_4$(aq)	HSe^-

Table 10 Results of solubility and speciation analysis for U, Np and Se in the natural barrier (oxidizing conditions)

element	Uranium	Neptunium	Selenium
conditions	Model 2A Eh : 40→ 500 (mV) pH : 8.0 → 4.0 [CT] = $2.3x10^{-5}$ (mol/l)	Model 2A Eh : 82→ 500 (mV) pH : 7.4 → 4.0 [CT] = $2.3x10^{-5}$ (mol/l)	Eh : -3→ 500 (mV) pH : 9.5 → 4.0
	Model 2B Eh : 66 → 500 (mV) pH : 7.6 → 4.0 [CT] = $4.4x10^{-3}$ (mol/l)	Model 2B Eh : 77 → 500 (mV) pH : 7.4 → 4.0 [CT] = $4.4x10^{-3}$ (mol/l)	
solubility (mol/l)	Model 2A $6x10^{-8}$ - $1x10^{-3}$	Model 2A $2x10^{-8}$ - $3x10^{-2}$	$2x10^{-3}$ - $1x10^{-2}$
	Model 2B $9x10^{-6}$ - $1x10^{-3}$	Model 2B $4x10^{-8}$ - $3x10^{-2}$	
solid phase	$U_4O_{9(c)} \rightarrow U_3O_{7(c,\beta)} \rightarrow U_3O_{8(c)} \rightarrow$schoepite	$Np(OH)_4$(s)	Se(c)
dominant species	Model 2A $UO_2(OH)_2$(aq)→UO_2^{2+}	Model 2A NpO_2^+	$SeO_3^{2-} \rightarrow HSeO_3^-$
	Model 2B $UO_2(CO_3)_n^{2-2n}$ (n=1-3) →UO_2^{2+}	Model 2B $NpO_2CO_3^- \rightarrow NpO_2^+$	

REFERENCES

(1) SKI, Swedish Nuclear Power Inspectorate :SKI Project-90, SKI Technical Report 91:23 (1991).

(2) Bruno, J., et al. : Radionuclide solubilities to be used in SKB 91, SKB-TR-92-13 (1992).

(3) Parkhurst, D. L., et al. : PHREEQE-A Computer Program for Geochemical Calculations, U. S. Geol. Surv. Water-Resour. Invest. 80-96, NTIS PB 81-167801 (1980).

(4) Wolery, T. J. : Calculation of Chemical Equibrium between Aqueous Solution and Minerals : The EQ3/6 Software Package, UCRL-52658 (1979).

(5) Wolery, T. J. : EQ3/6-A Computer Program for Geochemical Aqueous Speciation-Solubility Calculations : User's Guide and Documentation, UCRL-53414 (1983).

(6) Wolery, T. J., Daveler, S. A. : EQ6-A computer program for reaction path modelling of aqueous geochemical systems: User's guide and documentation (1989).

(7) PNC, Power Reactor and Nuclear Fuel Development Co. : Technical Report on Research and Deveopment of Geological Disposal for High Level Radioactive Waste -H3 (in Japanese) PNC TN 1410 92-081 (1992).

(8) Noma, Y. and Goto, H. : Groundwater in Ochigata Plain, Ishikawa Prefecture (in Japanese), Monthly Report of the Geological Survey, 21, 9 (1970).

(9) Snellman, M., et al. : Laboratory and Modelling Studies of Sodium Bentonite Groundwater Interaction, Scientific Basis for Nuclear Waste Management X, Materials Research Society, 781-790 (1987).

(10) OECD/NEA, OECD Nuclear Energy Agency :The NEA Thermochemical Data Base (TDB), (1983).

(11) OECD/NEA : Chemical Thermodynamics Vol. 1, "Chemical Thermodynamices of Uranium ", Wanner, H. and Forest, I. eds., Rorth-Holland (1992).

(12) Lemire, R. J. and Garisto, F.: The Solubility of U, Pu, Th and Tc in a Geological Disposal Vault for Used Nuclear Fuel, AECL-10009 (1989).

(13) Phillips, S. L., et al. : Thermodynamic tables for nuclear waste isolation: Reference values and neptunium, LBL-23733 (1987).

(14) Brown, P. L. and Wanner, H., : Predicted formation constants using the unified theory of metal ion complexation, OECD/NEA (1987).

(15) Wanner, H., : Modelling interaction of deep groundwater with bentonite and radionuclide speciation, EIR-Bericht Nr. 589 and Nagra NTB 86-21 (1986).

(16) Rai, D. and Ryan, J. L. : Neptunium(IV) hydrous oxide solubility under reducing and carbonate conditions, Inorg. Chem., 24, 3 (1985).

(17) Neck, V., Kim, J. I., et al. : Solubility and Hydrolysis Behaviour of Nepunium(V), Radiochim. Acta, 56 (1992).

(18) Baes, C. F., et al. : The hydrolysis of cations, New York: Wiley & Sons (1976).

(19) Moskvin, A. I. : Some thermodynamic characteristics of actinide compounds in a solid form, Sov. Radiochem., 15, 356-363 (1973).

(20) Wagman, D. D., et al. : The NBS tables of chemical thermodynamic properties, "Selected values for inorganic and C1 and C2 organic substances in SI units", J. Phys. Chem. Ref. Data, 11, supp 2 (1982).

(21) Zhdanov, S. I. : Standard potentials in aqueous solution, "Sulfur, selinium, tellurium and polonium", New York: Marcel Dekker, 93-126 (1985).

(22) Naumov, G. B., et al. : Handbook of thermodynamic data, Moscow: Atomizdat (1971).

(23) Mills, K. C. : Thermodynamic data for inorganic sulphides, selenides and tellurides, London: Butterworths (1974).

(24) Lindemer, T. B., et al. : Thermodynamic review and calculations, "Alkali-metal oxide systems with nuclear fuels, fission products, and structural materials, J. Nucl. Mat., 100, 178-226 (1981).

(25) Kubaschewski, O. and Alcock, C. B., : Metallurgical thermochemistry, 5th ed, Oxford: Pergamon Press, (1979).

(26) Tachikawa, H. : Standard potentials in aqueous solution, "Lithium, sodium, potassium, rubidium, cesium and francium", New York: Marcel Dekker, 727-762 (1985).

(27) Rai, D., et al. : The Solubility of Th(IV) and U(IV) Hydrous Oxides in Concentrated $NaHCO_3$ and Na_2CO_3 Solutions, Scientific Basis for Nuclear Waste Management XVIII, Materials Research Society, 1143-1150 (1994).

(28) Pratopo, M. I. , Moriyama, H. and Higashi, K. : Carbonate Compexation of Neptunium(IV) and Analogous Comlexation of Ground-Water Uranium, Radiochim. Acta, 51 (1990).

(29) Eriksen, T. E., et al. : Solubility of Redox-Sensitive Radionuclides ^{99}Tc and ^{237}Np under Reducing Conditions in Neutral to Alkaline Solutions. Effect of Carbonate, SKB-TR-93-18 (1993).

(30) Puigdomenech, I. and Bruno, J. : Modelling uranium solubilities in aqueous solutions: Validation of a thermodynamic data base for the EQ3/6 geochemical codes, SKB Technical Report 88-21 (1988).

(31) Robins, R. G. : Hydrolysis of uranyl nitrate solutions at elevated temperatures, J. Inorg. Nucl. Chem. 28, 119-123 (1966).

(32) Garisto, N. C. and Garisto, F. : The dissolution of UO_2: A thermodynamic approach, Nucl. Chem. Waste Management 6, 203-211 (1986).

(33) Strickert, R. G., Rai, D., and Fulton, R. W. : Effect of Aging on the Solubility and Crystallinity of Np(IV) Hydrous Oxide, Geochemical Behavior of Disposed Radioactive Waste, Am. Chem. Soc., Washington D. C., 135-145 (1984).

(34) Vuorinen, U., et al. : Solubility and speciation calculations (EQ3/6) for the elements of importance in TVO-92, YJT-92-11 (1992).

(35) Thomason, H. P. : The Study of Actinide Solubility Limiting Solid Phases-A Literature Survey, DOE/RW/88.094, AERE-R 12995 (1988).

(36) Elrashidi, M. A., et al. : Chemical Equilibria of Selenium in soils: A Theoretical Development, Soil Science, 144, 2, 141-152 (1987).

(37) Rai, D., Felmy, A. R. and Ryan, J. L. : Uranium(IV) Hydrolysis Constants and Solubility Product of $UO_2 \cdot xH_2O$(am), Inorg. Chem., 29, 260-264 (1990).

(38) Bruno, J. et al. : The Determination of the Solubility of Amorphous UO_2(s) and the Mononuclear Hydrolysis Constants of Uranium(IV) at 25 ℃, Scientific Basis for Nuclear Waste Management X, Materials Research Society, 153-160 (1987).

Appendix

Thermodynamics Data for Uranium, Neptunium, and Selenium.

NOTATION

ΔG° : the standard molar Gibbs energy of formation

ΔH° : the standard molar enthalpy of formation

S° : the standard molar entropy

Cp : the standard molar heat capacity

Table 1 Thermodynamic data for Uranium species (298.15K,0.1MPa,ionic strength I=0 M)

Species	ΔG° (kcal/mol)	ΔH° (kcal/mol)	S° (cal/mol/K)	Cp (cal/mol/K)	References
U^{3+}	-113.890	-110.908	-44.978	-15.298	(11)
U^{4+}	-126.651	-141.313	-99.649	-11.473	(11)
UO_2^{+}	-229.710	-245.033	-5.976		(11)
UO_2^{2+}	-227.685	-243.568	-23.472	10.135	(11)
UOH^{3+}	-182.597	-198.421	-47.792		(11)
UO_2OH^{+}	-277.273	-301.570	4.063		(11)
$UO_2(OH)_2(aq)$	-326.997				(11)
$U(OH)_4(aq)$	-347.186	-395.780	9.561	49.0	(11)
$UO_2(OH)_3^{-}$	-371.537				(11)
$U(OH)_5^{-}$	-387.497				(11)
$UO_2(OH)_4^{2-}$	-409.392				(11)
$(UO_2)_2OH^{3+}$	-508.369				(11)
$(UO_2)_2(OH)_2^{2+}$	-561.068	-614.792	-9.083		(11)
$(UO_2)_3(OH)_4^{2+}$	-893.550				(11)
$(UO_2)_3(OH)_5^{+}$	-945.253	-1049.108	19.839		(11)
$(UO_2)_3(OH)_7^{-}$	-1037.539				(11)
$(UO_2)_4(OH)_7^{+}$	-1277.639				(11)
UCl^{3+}	-160.362	-185.791	-93.482		(11)
UO_2Cl^{+}	-259.281	-281.592	-2.752		(11)
$UO_2Cl_2(aq)$	-288.913	-319.856	10.577		(11)
$UO_2ClO_3^{+}$	-230.256	-269.359	14.483		(11)
USO_4^{2+}	-313.465	-356.757	-58.703		(11)
$UO_2SO_3(aq)$	-353.209				(11)
$UO_2SO_4(aq)$	-409.819	-456.264	10.998		(11)
$U(SO_4)_2(aq)$	-496.664	-568.209	-16.495		(11)
$UO_2(SO_4)_2^{2-}$	-589.007	-669.891	32.456		(11)
UNO_3^{3+}	-155.139				(11)
$UO_2NO_3^{+}$	-254.577				(11)
$U(NO_3)_2^{2+}$	-182.754				(11)
$UO_2CO_3(aq)$	-367.074	-403.771	12.882		(11)
$UO_2(CO_3)_2^{2-}$	-503.161	-561.942	44.976		(11)
$UO_2(CO_3)_3^{4-}$	-635.701	-737.132	8.092		(11)

Table 1 (continued)

Species	ΔG° (kcal/mol)	ΔH° (kcal/mol)	S° (cal/mol/K)	Cp (cal/mol/K)	References
$UO_2(CO_3)_3^{5-}$	-618.360				(11)
$U(CO_3)_4^{4-}$	-679.296				(11)
$U(CO_3)_5^{6-}$	-803.949	-953.083	-19.851		(11)
$(UO_2)_3(CO_3)_6^{6-}$	-1513.823	-1714.079	54.719		(11)
$(UO_2)_2CO_3(OH)_3^-$	-750.430				(11)
$(UO_2)_3O(OH)_2(HCO_3)^+$	-980.175				(11)
uraninite(=UO_2(c))	-246.636	-259.344	18.412	15.202	(11)
U(c)	0.0	0.0	11.999	6.611	(11)
α-UO_3	-272.591	-291.015	23.759	19.562	(11)
β-UO_3	-273.040	-291.684	23.023	19.442	(11)
γ-UO_3	-273.862	-292.521	22.973	19.521	(11)
α-UO_3 · 0.9H_2O	-328.556	-360.046	30.117	33.464	(11)
β-$UO_2(OH)_2$	-334.322	-366.619	32.986	33.703	(11)
schoepite(=UO_3 · 2H_2O)	-391.168	-436.486	45.066	41.129	(11)
U_4O_9(c)	-1022.197	-1078.488	79.864	70.121	(11)
β-U_4O_9(c)	-1022.157	-1077.914	81.651		(11)
β-U_3O_7(c)	-774.856	-818.905	59.883	50.964	(11)
U_3O_8(c)	-805.393	-854.472	67.535	56.872	(11)
UCl_3(c)	-190.290	-206.447	37.790	22.731	(11)
UCl_4(c)	-222.193	-243.520	47.112	29.161	(11)
UCl_5(c)	-222.322	-248.349	58.012	35.997	(11)
UCl_6(c)	-224.018	-254.922	68.314	41.997	(11)
UOCl(c)	-187.792	-199.324	24.500	16.971	(11)
$UOCl_2$(c)	-238.663	-255.591	33.062	22.722	(11)
$UOCl_3$(c)	-249.920	-272.490	40.802	28.014	(11)
UO_2Cl(c)	-261.795	-279.924	26.890	21.034	(11)
UO_2Cl_2(c)	-273.886	-297.253	35.983	25.781	(11)
$U_2O_2Cl_5$(c)	-486.970	-525.240	77.990	52.440	(11)
$(UO_2)_3Cl_3$(c)	-534.180	-574.740	65.970	48.670	(11)
$U_5O_{12}Cl$(c)	-1318.950	-1399.360	111.150		(11)
UO_2Cl_2 · H_2O	-335.830	-372.830	46.010		(11)
UO_2ClOH · 2H_2O	-425.998	-480.539	56.410		(11)

Table 1 (continued)

Species	ΔG° (kcal/mol)	ΔH° (kcal/mol)	S° (cal/mol/K)	Cp (cal/mol/K)	References
$UO_2Cl_2 \cdot 3H_2O$	-452.863	-517.445	65.015		(11)
US(c)	-76.711	-77.014	18.642	12.080	(11)
US_2(c)	-124.112	-124.389	26.393	17.841	(11)
US_3(c)	-128.418	-128.979	33.103	22.851	(11)
U_2S_3(c)	-210.292	-210.104	47.614	31.958	(11)
U_3S_5(c)	-340.631	-342.047	69.557		(11)
UO_2SO_3(c)	-365.799	-397.023	37.527		(11)
UO_2SO_4(c)	-402.945	-441.038	39.009	34.659	(11)
$U(SO_3)_2$(c)	-409.411	-450.087	38.005		(11)
$U(SO_4)_2$(c)	-498.256	-552.056	43.025		(11)
$U(OH)_2SO_4$(c)	-422.174				(11)
$UO_2SO_4 \cdot 2.5H_2O$	-549.397	-623.142	58.814		(11)
$UO_2SO_4 \cdot 3H_2O$	-577.622	-657.682	65.515		(11)
$UO_2SO_4 \cdot 3.5H_2O$	-606.075	-693.560	68.487		(11)
$U(SO_4)_2 \cdot 4H_2O$	-725.041	-832.577	85.811		(11)
$U(SO_4)_2 \cdot 8H_2O$	-953.213	-1114.485	128.596		(11)
$UO_2(NO_3)_2$(c)	-264.386	-322.925	57.605		(11)
$UO_2(NO_3)_2 \cdot H_2O$	-325.785	-397.740	68.362		(11)
$UO_2(NO_3)_2 \cdot 2H_2O$	-387.343	-472.962	78.287	66.449	(11)
$UO_2(NO_3)_2 \cdot 3H_2O$	-445.711	-545.076	87.938	76.512	(11)
$UO_2(NO_3)_2 \cdot 6H_2O$	-617.695	-757.117	120.852	111.864	(11)
UO_2CO_3(c)	-373.610	-403.870	34.468	28.707	(11)
$USiO_4$(c)	-450.230	-475.980	28.205		(11)
$MgUO_4$(c)	-418.201	-443.944	31.540	30.619	(11)
$CaUO_4$(c)	-451.451	-478.603	28.946	29.591	(11)
$NaUO_3$(c)	-337.624	-357.321	31.752	26.023	(11)
α -Na_2UO_4	-425.301	-453.601	39.678	35.065	(11)
$Na_2U_2O_7$(c)	-719.818	-765.793	65.947	54.331	(11)
Na_3UO_4(c)	-454.129	-483.790	47.375	41.352	(11)
$Na_4UO_2(CO_3)_3$(c)	-893.442				(11)
K_2UO_4(c)	-429.889	-459.098	43.025		(11)

Table 2 Thermodynamic data for Neptunium species (298.15K,0.1MPa,ionic strength I=0 M)

Species	ΔG° (kcal/mol)	ΔH° (kcal/mol)	S° (cal/mol/K)	Cp (cal/mol/K)	References
Np^{3+}	-123.612	-126.003	-42.810		(12)
$NpOH^{2+}$	-170.737	-182.353	-17.927		(13)
$Np(OH)_2^{+}$	-216.513				(13)
$Np(OH)_3(aq)$	-257.956				(14)
$Np(OH)_4^{-}$	-302.591				(15)
$Np(OH)_5^{2-}$	-341.728				(14)
Np^{4+}	-120.222	-132.914	-92.981		(12)
$NpOH^{3+}$	-175.446	-188.944	-39.917		(12)
$Np(OH)_2^{2+}$	-229.697	-251.049	-10.517		(12)
$Np(OH)_4(aq)$	-333.889	-380.007	17.927		(12)
$Np(OH)_5^{-}$	-370.879				(16)
NpO_2^{+}	-218.706	-233.816	-5.020		(12)
$NpO_2OH(aq)$	-263.153	-291.554	5.976		(12)
$NpO_2(OH)_2^{-}$	-299.795				(17)
$NpO_2(OH)_3^{2-}$	-341.165				(14)
$NpO_2(OH)_4^{3-}$	-380.248				(14)
NpO_2^{2+}	-190.217	-205.677	-21.990		(12)
NpO_2OH^{+}	-239.942	-263.027	8.189		(15)
$NpO_2(OH)_2(aq)$	-289.394	-325.346	20.786		(15)
$NpO_2(OH)_3^{-}$	-334.343				(15)
$NpO_2(OH)_4^{2-}$	-383.672				(14)
$(NpO_2)_2(OH)_2^{2+}$	-485.201	-537.251	-3.346		(12)
$(NpO_2)_3(OH)_5^{+}$	-830.320	-931.879	27.727		(12)
$NpCO_3^{+}$	-259.713				(14)
$Np(CO_3)_2^{-}$	-393.876				(14)
$Np(CO_3)_3^{3-}$	-526.471				(14)
$Np(CO_3)_5^{6-}$	-803.286	-935.117	38.244		(12)
$NpO_2CO_3^{-}$	-351.107	-382.066	47.850		(12)
$NpO_2(CO_3)_2^{3-}$	-480.640	-549.666	26.293		(12)
$NpO_2(CO_3)_3^{5-}$	-596.610				(13)
$NpO_2CO_3(aq)$	-327.560				(14)

Table 2 (continued)

Species	DG° (kcal/mol)	DH° (kcal/mol)	S° (cal/mol/K)	Cp (cal/mol/K)	References
$NpO_2(CO_3)_2^{2-}$	-461.999	-522.093	40.635		(12)
$NpO_2(CO_3)_3^{4-}$	-598.610				(12)
$(NpO_2)_3(CO_3)_6^{6-}$	-1409.742				(15)
$NpSO_4^{2+}$	-305.699	-348.699	-56.228		(13)
$Np(SO_4)_2(aq)$	-489.495	-558.066	-6.454		(12)
$NpO_2SO_4^{-}$	-397.235	-446.644	16.732		(12)
$NpO_2SO_4(aq)$	-372.147	-418.062	12.832		(13)
$NpO_2(SO_4)_2^{2-}$	-552.439	-634.329	28.611		(13)
$NpCl^{3+}$	-152.029	-168.133	-62.147		(12)
$NpCl_2^{2+}$	-182.855	-190.186	9.561		(12)
$NpO_2Cl(aq)$	-249.532	-270.074	19.122		(13)
NpO_2Cl^{+}	-221.331	-242.741			(13)
$NpO_2Cl_2(aq)$	-252.158	-280.928	17.640		(13)
$Np(OH)_4(s)$	-344.918				(16)
$NpO_2OH(s)$	-269.178				(17)
$NpO_2OH(am)$	-268.249				(17)
$NpO_2(OH)_2(c)$	-295.413	-329.154	28.205		(12)
$NpO_2(OH)_2(am)$	-294.579				(18)
$Np_2O_5(c)$	-481.141	-513.250	-38.961		(13)
$NpO_2CO_3(c)$	-335.227	-361.105	49.233		(15)
$NaNpO_2CO_3 \cdot 3.5H_2O$	-621.648	-701.664	75.054		(12)
$Np(SO_4)_2(c)$	-342.094	-397.979	36.093		(19)
$NpCl_3(c)$	-219.207				(14)
$NpCl_4(c)$	-250.755				(14)
$NpOCL_2(c)$	-231.309	-248.014	33.703		(13)

Table 3 Thermodynamic data for Selenium species (298.15K,0.1MPa,ionic strength I=0 M)

Species	ΔG° (kcal/mol)	ΔH° (kcal/mol)	S° (cal/mol/K)	Cp (cal/mol/K)	References
Se^{2-}	30.906				(20)
HSe^-	10.517	3.801	18.883		(20)
H2Se(aq)	5.306	4.589	39.105		(20)
SeO_3^{2-}	-88.392	-121.712	3.107		(20)
$HSeO_3^-$	-98.350	-122.991	32.292		(20)
H2SeO3(aq)	-101.859	-122.991	49.694		(20)
SeO_4^{2-}	-105.482	-143.201	12.907		(20)
$HSeO_4^-$	-108.088	-139.018	35.711		(20)
H2SeO4(aq)	-105.483	-143.201	12.931		(21)
Na2Se(aq)	-94.320				(20)
Na2SeO3(aq)	-213.618	-236.517	31.073		(20)
NaHSeO3(aq)	-160.949	-180.386	46.395		(20)
Na2SeO4(aq)	-230.708	-258.029	41.113		(20)
NaHSeO4(aq)	-170.689	-196.408	49.813		(20)
K2Se(aq)	-104.502				(20)
KHSe(aq)	-57.199	-56.506	43.025		(20)
K2SeO3(aq)	-223.801	-242.325	52.108		(20)
K2SeO4(aq)	-240.915	-263.814	61.908		(20)
KHSeO4(aq)	-175.804	-199.324	60.211		(20)
MgSeO4(aq)	-214.192	-254.826	-20.102		(20)
NH4HSe(aq)	-5.569	-31.814	23.114		(20)
(NH4)2Se(aq)	-6.956				(20)
NH4HSeO3(aq)	-117.305	-154.665	59.398		(20)
(NH4)2SeO3(aq)	-126.254	-185.007	56.888		(20)
NH4HSeO4(aq)	-127.067	-170.713	62.816		(20)
(NH4)2SeO4(aq)	-143.368	-206.519	67.095		(20)
Se(c)	0.0	0.0	10.145	6.062	(20)
Se(am)	0.645	1.291	12.310		(21)
SeO2(c)	-41.487	-53.865	17.627		(21)
SeO3(c)	-20.102	-39.903	17.301		(22)
Se2O5(c)	-67.570	-98.814	38.005		(23)
NaSe(c)	-44.208	-46.050	15.001		(25)

Table 3 (continued)

Species	ΔG° (kcal/mol)	ΔH° (kcal/mol)	S° (cal/mol/K)	Cp (cal/mol/K)	References
$Na_2Se(c)$	-78.126	-81.891	22.0		(24)
$Na_2Se_2(c)$	-88.385	-92.742	30.117		(23)
$Na_2SeO_4(c)$	-231.912	-261.352	27.966		(26)
$K_2Se(c)$	-88.715	-92.001	29.998		(24)
$K_2SeO_3(c)$	-209.856	-231.019	43.598		(24)
$K_2SeO_4(c)$	-239.696	-265.324	53.064		(20)
CaSe(c)	-86.814	-88.010	16.015		(20)
$CaSeO_4 \cdot 2H_2O$	-355.385	-407.947	53.064		(20)
$CaSeO_3 \cdot 2H_2O$	-341.497				(20)
MgSe(c)	-68.945	-69.796	15.059		(23)
$MgSeO_3(c)$	-194.737	-215.169	22.902		(25)
$MgSeO_3 \cdot 6H_2O$	-541.754	-645.754	76.895		(26)
FeSe(c)	-18.094	-18.002	16.871		(22)
$FeSe_2(c)$	-23.220	-25.002	20.759	17.423	(23)
$Fe_3Se_4(c)$	-52.748	-50.717	66.882	52.626	(23)
$Fe(SeO_3)_3 \cdot 2H_2O$	-438.829				(22)
$Al_2Se_3(c)$	-127.122	-129.012	37.503		(25)
$NH_4HSe(c)$	-5.569	-31.814	23.114		(20)
$SeCl_4(c)$	23.320	-43.813	-108.420		(21)